

Politecnico di Torino

Politecnico di Torino

Master of Science's Degree in Biomedical Engineering

A.a. 2025/2026

Graduation Session September 2026

Performance evaluation of the inertial-based digital mobility MobGap pipeline for gait parameter estimation in people with ataxia

Supervisors:
Prof. Andrea CEREATTI
Dr. Tecla BONCI
Dr. Rachele ROSSANIGO

Candidate:
Milena GATTINO

Abstract

Ataxia is a neurological condition characterised by impaired coordination and balance, leading to gait alterations and an increased risk of falls. Parameters measured during standardised clinical tests may not fully represent how patients move in daily life and gait alterations may be difficult to capture through clinical observation alone. Sensor-based gait assessment instead provides an objective way to quantify gait and monitor disease progression both in clinics and in real-world scenarios. Recently, a pipeline based on a single lumbar on inertial measurement unit (IMU) (i.e., MobGap) has been validated for gait assessment in real-world conditions in different pathological populations, but people with ataxia were not included. This thesis investigates whether a single lower-back inertial device can correctly detect strides and accurately estimate key digital gait parameters (i.e., stride duration, stride length, and stride velocity) in people with ataxia during standardised and unstructured walking tests. Five adults with ataxia (age: 60±5 years) were enrolled at the Royal Hallamshire Hospital in Sheffield and were asked to perform three standardised clinical tests and an unstructured walking test in the hospital. Participants wore a lumbar-mounted IMU (Axivity) and a portable multi-sensor system (INDIP), used as reference. MobGap pipeline was applied to the Axivity data to detect strides and extract gait parameters. These estimates were compared to reference INDIP parameters. Firstly, using the detected foot-to-ground contacts, sensitivity and positive predictive values were quantified. Gait parameters errors were then assessed for strides concurrently detected by both systems, with analyses stratified by walking condition (straight walking vs. turning) and rollator use. Overall, 4151 reference strides were detected compared to 3921 identified by the single-sensor approach. A total of 69% were concurrently detected and subsequently analysed for error assessment, with 83% classified as straight strides and 8% as turning strides. The analysis included walking bouts with durations ranging from 3 to 360 s. Gait parameter estimation was less accurate during turns: errors increased from 2.2% during straight walking to 4.0% in turns for stride duration, from 13% to 40% for stride length, and from 13% to 38% for walking speed. The use of a rollator negatively affected both stride detection and gait parameter estimation. Sensitivity and positive predictive value decreased from 99% to 54% and from 97% to 55%, respectively. Stride duration error slightly increased from 2% to 3%. In contrast, spatio-temporal errors increased substantially from 9% to 27% for stride length and 8% to 27% for walking speed. Averaging all strides, MobGap showed performance in people with ataxia that was comparable to or exceeded that reported in healthy individuals and other clinical populations. However, these preliminary findings provide a basis for developing recommendations

for the analysis of gait features obtained during prolonged real-world monitoring. In particular, they highlight that caution should be exercised when aggregating data across all walking episodes, as sensor performance may vary depending on walking conditions.

Acknowledgements

I would like to express my sincere gratitude to everyone who supported me and contributed to this thesis project, making this experience both professionally and personally meaningful.

In particular, I would like to thank Prof. Andrea Cereatti for giving me the opportunity to undertake this experience and for encouraging me.

I am grateful to Tecla Bonci for her continuous support during my time in Sheffield, for her careful guidance, and for making me feel welcome from the very beginning.

I would also like to thank Rachele Rossanigo for supporting me during my time in Turin, from the initial stages of the project and throughout the entire thesis work.

I would like to thank my fellow thesis students for sharing this experience with me and for making these months of work both enjoyable and memorable.

Finally, I would like to thank my family for always supporting me and for standing by every decision that my university journey has led me to make.

Table of Contents

List of Tables VI

List of Figures VII

Glossario X

1 Introduction 1
- 1.1 Ataxia: clinical features . . . 1
- 1.2 Clinical relevance of gait assessment in ataxia . . . 2
- 1.3 From clinical gait assessment to wearable monitoring . . . 3
- 1.4 Aim and objectives of the thesis . . . 4
  - 1.4.1 Thesis outline . . . 5

2 Background and state of the art 6
- 2.1 Fundamentals of gait analysis . . . 6
  - 2.1.1 Physiological gait . . . 7
  - 2.1.2 Ataxic gait . . . 9
- 2.2 Technologies for gait analysis . . . 10
  - 2.2.1 Optoelectronic Motion Capture System . . . 10
  - 2.2.2 Force platform . . . 11
  - 2.2.3 Pressure insoles . . . 12
  - 2.2.4 MIMU . . . 13
- 2.3 Free-living gait assessment . . . 16
  - 2.3.1 Gait capacity vs gait performance . . . 17
  - 2.3.2 Relevance of free-living gait assessment in ataxia . . . 17
- 2.4 Current limitations and research gap . . . 18

3 Materials 20
- 3.1 INDIP reference system . . . 20
  - 3.1.1 INDIP MIMUs . . . 22
  - 3.1.2 INDIP pressure insoles . . . 23

3.1.3 INDIP distance sensors . . . 23
3.2 Axivity sensor . . . 25
3.3 Overview of data collection . . . 26
3.4 Experimental protocol . . . 26
3.5 7-day data collection . . . 30

4 Data Processing and Methods 31
4.1 Data preparation . . . 31
4.1.1 Temporal alignment between INDIP and Axivity . . . 31
4.1.2 Data organisation . . . 33
4.1.3 Lower-back sensor reorientation . . . 33
4.2 Processing . . . 34
4.2.1 Turn detection . . . 35
4.3 Stride matching . . . 36
4.3.1 Initial contact matching . . . 36
4.3.2 Stride matching . . . 36
4.4 Performance evaluation . . . 38
4.4.1 Stratification by rollator use . . . 38
4.4.2 Stratification by walking condition: straight and turning strides 39
4.5 Free-living data processing . . . 40
4.5.1 CWA file reading and daily segmentation . . . 40
4.5.2 Daily MobGap processing . . . 40
4.5.3 Free-living data analysis . . . 41

5 Results 43
5.1 Axivity temporal alignment . . . 43
5.2 MobGap performance . . . 44
5.2.1 Participant-specific performance . . . 44
5.2.2 Stratification by rollator use . . . 44
5.2.3 Overall gait-parameter estimation performance . . . 44
5.2.4 Straight and turning strides . . . 47
5.3 MobGap performance after sensor reorientation . . . 49
5.3.1 Participant-specific performance . . . 49
5.3.2 Overall gait-parameter estimation performance . . . 49
5.4 7-day recordings . . . 52
5.4.1 Participant S1 – 0239 . . . 52
5.4.2 Participant S2 – 807 . . . 55
5.4.3 Participant S5 – 180 . . . 55
5.4.4 Overall turn distribution . . . 60

6 Discussion 61
6.1 Overall MobGap performance in people with ataxia 61
6.2 Influence of rollator use and walking condition on MobGap performance 63
6.3 Effect of lower-back sensor reorientation 64
6.4 Free-living gait assessment 66

7 Conclusion 69
7.1 General results 69
7.2 Further improvements 70

Bibliography 71

List of Tables

3.1 Participant characteristics and data availability. 27

5.1 Participant-specific stride-detection performance using the original sensor orientation. Mean trunk inclination was calculated across the available walking trials. TP: true positives; FN: false negatives; FP: false positives; PPV: positive predictive value. 45

5.2 Participant-specific gait-parameter estimation errors using the original sensor orientation. Bias and absolute relative error (ARE) are reported as median [Q1–Q3]. 46

5.3 Overall gait-parameter estimation performance using the original sensor orientation. ARE and bias are reported as median [Q1–Q3]. . 47

5.5 Overall gait-parameter estimation performance for straight and turning strides using the original sensor orientation. ARE is reported as median [Q1–Q3]. 47

5.4 Participant-specific gait-parameter estimation errors for straight and turning strides using the original sensor orientation. Only correctly matched strides were included and intermediate strides were excluded. Absolute relative error (ARE) is reported as median [Q1–Q3]. N_{SD} indicates the number of valid stride-duration estimates, while $N_{SL/WS}$ indicates the number of valid stride-length and walking-speed estimates. 48

5.8 Overall gait-parameter estimation performance after lower-back sensor reorientation. Absolute relative error (ARE) is reported as median [Q1–Q3]. MARE: mean absolute relative error. 49

5.6 Participant-specific stride-detection performance after lower-back sensor reorientation. Mean trunk inclination was calculated across the available walking trials. TP: true positives; FN: false negatives; FP: false positives; PPV: positive predictive value. 50

5.7 Participant-specific gait-parameter estimation errors after lower-back sensor reorientation. Bias and absolute relative error (ARE) are reported as median [Q1–Q3]. 51

List of Figures

1.1 Anatomical position of the cerebellum, located inferior to the cerebrum and posterior to the pons. Reproduced from TeachMeAnatomy, TeachMeSeries Ltd. (2026). 1

2.1 Schematic representation of step and stride during walking. 7
2.2 Human movement analysis laboratory showing the main measurement systems and their reference frames. Reproduced from Cappozzo et al. [16]. 11
2.3 Example of a force platform used for the measurement of ground reaction forces during gait analysis. Reproduced from Auptimo [17]. 12
2.4 Main sensing components of a Magneto-Inertial Measurement Unit (MIMU), combining a tri-axial accelerometer, gyroscope, and magnetometer. 13
2.5 Mass–spring–damper representation of a MEMS accelerometer. An applied acceleration produces a relative displacement of the proof mass with respect to the sensor frame. Reproduced from Mohammed et al. [21]. 14

3.1 Complete INDIP configuration and positioning of the pressure insoles, foot-mounted MIMUs, lower-back MIMU, and distance sensors. Adapted from Salis et al. [19]. 21
3.2 Conventional positioning and orientation of the INDIP sensors with respect to the anatomical axes. 22
3.3 Distribution of the 16 force-sensitive resistor elements in the INDIP pressure insole. The sensing elements cover the forefoot, midfoot, and rearfoot regions. Adapted from Salis et al. [18]. 23
3.4 Operating principle of the infrared Time-of-Flight proximity sensor. The distance from the reflecting target is estimated by measuring the phase shift between the emitted and reflected signals. Reproduced from Bertuletti et al. [31]. 24
3.5 Axivity AX6 wearable inertial sensor used in this study. 25

3.6 Schematic overview of the four walking tests included in the performance evaluation: Timed Up and Go, performed twice; 10-m Straight Walk, performed twice; 6-Minute Walk Test, performed once by continuously walking back and forth along a 10-m walkway; and Unstructured Walk, performed once within the hospital corridors. 29

3.7 Experimental sensor setup used during data collection. 29

4.1 Hierarchical organisation of the INDIP and Axivity data within the `data.mat` file. For each test and trial, the multi-sensor INDIP data were stored in the `SU_INDIP` structure, whereas the single-sensor Axivity data were stored in the `SU` structure. 33

5.1 Temporal alignment between the Axivity sensor and the INDIP reference system. 43

5.2 Cumulative distribution of walking bouts according to turn percentage for participant S1 (0239). Each series represents one recording day. The first point includes only walking bouts with 0% detected turning, while subsequent thresholds progressively include walking bouts with increasing turn percentages up to 100%. The vertical axis represents the percentage of walking bouts relative to the total number detected on each day. 53

5.3 Stride duration for participant S1 (0239). Clinical distributions are shown for INDIP and MobGap. Daily-life distributions include all MobGap strides and the subset belonging to walking bouts with 0% detected turning. 53

5.4 Stride length for participant S1 (0239). Clinical distributions are shown for INDIP and MobGap. Daily-life distributions include all MobGap strides, strides from walking bouts with 0% detected turning, and the subset of 0%-turn walking bouts lasting at least 10 s. 54

5.5 Walking speed for participant S1 (0239). Clinical distributions are shown for INDIP and MobGap. Daily-life distributions include all MobGap strides, strides from walking bouts with 0% detected turning, and the subset of 0%-turn walking bouts lasting at least 10 s. 54

5.6 Cumulative distribution of walking bouts according to turn percentage for participant S2 (807). Each series represents one recording day. Walking bouts are progressively included from those with 0% detected turning up to a maximum accepted turn percentage of 100%. The vertical axis represents the percentage of walking bouts relative to the total number detected on each day. 55

5.7 Stride duration for participant S2 (807). Clinical distributions are shown for INDIP and MobGap. Daily-life distributions include all MobGap strides and the subset belonging to walking bouts with 0% detected turning. 56
5.8 Stride length for participant S2 (807). Clinical distributions are shown for INDIP and MobGap. Daily-life distributions include all MobGap strides, strides from walking bouts with 0% detected turning, and the subset of 0%-turn walking bouts lasting at least 10 s. 56
5.9 Walking speed for participant S2 (807). Clinical distributions are shown for INDIP and MobGap. Daily-life distributions include all MobGap strides, strides from walking bouts with 0% detected turning, and the subset of 0%-turn walking bouts lasting at least 10 s. 57
5.10 Cumulative distribution of walking bouts according to turn percentage for participant S5 (180). Each series represents one recording day. Walking bouts are progressively included from those with 0% detected turning up to a maximum accepted turn percentage of 100%. The vertical axis represents the percentage of walking bouts relative to the total number detected on each day. 57
5.11 Stride duration for participant S5 (180). Clinical distributions are shown for INDIP and MobGap. Daily-life distributions include all MobGap strides and the subset belonging to walking bouts with 0% detected turning. 58
5.12 Stride length for participant S5 (180). Clinical distributions are shown for INDIP and MobGap. Daily-life distributions include all MobGap strides, strides from walking bouts with 0% detected turning, and the subset of 0%-turn walking bouts lasting at least 10 s. 59
5.13 Walking speed for participant S5 (180). Clinical distributions are shown for INDIP and MobGap. Daily-life distributions include all MobGap strides, strides from walking bouts with 0% detected turning, and the subset of 0%-turn walking bouts lasting at least 10 s. 59
5.14 Overall cumulative distribution of free-living walking bouts according to the maximum accepted turn percentage. In the upper panel, points represent the median percentage of retained walking bouts across recording days for each participant, with error bars indicating the interquartile range. The lower panel reports the median across participant-level values, with the corresponding interquartile range. Each participant therefore contributes equally to the overall summary. 60

Glossario

SARA
: Scale for the Assessment and Rating of Ataxia

SF-12
: 12-Item Short Form Health Survey

PCS
: Physical Component Summary

EQ-VAS
: EuroQol Visual Analogue Scale

TUG
: Timed Up and Go

SW
: Straight Walk

6MWT
: 6-Minute Walk Test

UW
: Unstructured Walk

Pers
: Personalization

IC
: Initial Contact

SD

Stride Duration

SL

Stride Length

WS

Walking Speed

TP

True Positive

FN

False Negative

FP

False Positive

PPV

Positive Predictive Value

MAE

Mean Absolute Error

ARE

Absolute Relative Error

MARE

Mean Absolute Relative Error

DMO

Digital Mobility Outcome

INDIP

INertial module with DIstance sensors and Pressure insoles

PI

Pressure Insole

DS

Distance Sensor

IMU

Inertial Measurement Unit

MIMU

Magneto-Inertial Measurement Unit

MEMS

Micro-Electro-Mechanical Systems

GRF

Ground Reaction Force

CoP

Centre of Pressure

ICF

International Classification of Functioning, Disability and Health

CWA

Continuous Wave Accelerometer file format

Chapter 1

Introduction

1.1 Ataxia: clinical features

Ataxia is a neurological syndrome characterised by impaired coordination of voluntary movements. It is not a single disease, but a clinical manifestation that can result from different disorders affecting the nervous system. Although ataxia can also arise from sensory or vestibular dysfunction, it is most commonly associated with abnormalities of the cerebellum and its connections [1].

The cerebellum is located in the posterior part of the brain, behind the brainstem, as shown in Figure 1.1. It plays an important role in movement coordination and adaptation. Damage to the cerebellum or to its afferent and efferent pathways can therefore interfere with movement control without necessarily causing muscle weakness [2].

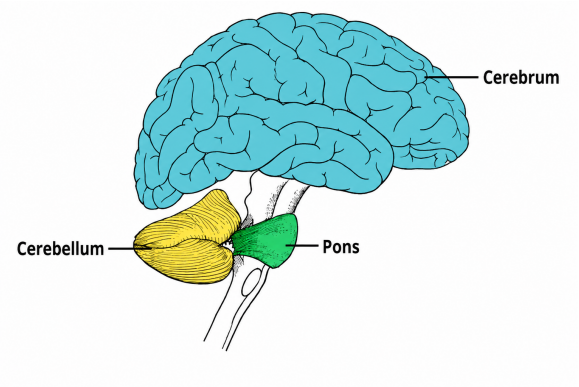


Figure 1.1: Anatomical position of the cerebellum, located inferior to the cerebrum and posterior to the pons. Reproduced from TeachMeAnatomy, TeachMeSeries Ltd. (2026).

The causes of ataxia are heterogeneous. Ataxias can be broadly classified as hereditary or acquired. Hereditary forms include autosomal dominant disorders, such as spinocerebellar ataxias, and autosomal recessive conditions, such as Friedreich ataxia. Acquired forms may instead result from vascular lesions, immune-mediated diseases, infections, nutritional deficiencies, toxic substances, medications, tumours, or other neurological conditions. In some patients, the underlying cause remains unknown despite diagnostic investigation [1, 2].

Age of onset and disease progression also vary between different forms of ataxia. Some hereditary conditions begin during childhood or adolescence, while several spinocerebellar ataxias become clinically evident in adulthood [3]. Acquired ataxias may occur at any age and can have an acute, subacute, or progressive course depending on the underlying cause [1].

Clinical manifestations depend on the structures involved and on disease severity. Common symptoms include impaired balance and gait, limb incoordination, dysmetria, intention tremor, dysarthria, and abnormalities of eye movements [2]. Gait impairment is particularly relevant because it directly affects mobility. People with ataxia may show instability, increased stride-to-stride variability, and difficulty maintaining a stable walking trajectory. With disease progression, some individuals may also require walking aids or external assistance [4].

1.2 Clinical relevance of gait assessment in people with ataxia

Gait and balance impairment are among the main motor problems in people with ataxia. In degenerative cerebellar ataxias, these disturbances can appear early and progressively affect mobility and daily activities [5]. Gait assessment is therefore useful for describing motor impairment and for monitoring changes over time.

Clinical evaluation is commonly based on neurological examination and standardised rating scales. One of the most widely used is the Scale for the Assessment and Rating of Ataxia (SARA), which evaluates gait, stance, sitting, speech, and limb coordination [6].

Clinical scales are essential for evaluating disease severity, but they provide a global score based on a limited number of predefined tasks. Quantitative gait analysis can add further information by measuring specific temporal and spatial characteristics of walking that are difficult to describe through clinical observation alone.

Digital gait and balance measures are therefore receiving increasing attention in ataxia research. Recent recommendations from the Ataxia Global Initiative support their use for characterising disease severity and monitoring progression, together with conventional clinical outcomes [5].

These measures, however, are useful only if they can be estimated reliably in the population in which they are applied. Ataxic gait is often irregular and variable. Changes in direction and the use of walking aids can further modify the walking pattern [4]. These conditions can also make automatic gait analysis more difficult. For this reason, the performance of a gait-analysis method should be evaluated specifically in people with ataxia before its outputs are used for clinical or research purposes.

1.3 From clinical gait assessment to wearable monitoring

Quantitative gait analysis can be performed using different measurement technologies. Laboratory-based systems provide detailed information under controlled conditions and remain important reference methods for biomechanical analysis. Their use, however, is generally limited to dedicated environments and relatively short recording sessions. The main technologies used for gait analysis are described in more detail in Chapter 2.

Wearable inertial sensors provide a less constrained alternative. They can be attached directly to the body and used to estimate temporal and spatial gait parameters from acceleration and angular-velocity signals. A setup based on a single sensor placed on the lower back is particularly interesting because it reduces the amount of instrumentation required and can also be used for prolonged recordings.

This becomes especially useful when gait assessment is extended beyond standard clinical tests. A prescribed walking task shows how a person performs under controlled conditions, but it does not necessarily represent how that person walks during everyday life. Daily walking includes changes in direction, different walking speeds, and walking episodes of different durations.

Wearable sensors make it possible to record these conditions over longer periods and in the person's usual environment. In people with degenerative cerebellar ataxia, gait measures obtained during real-life walking have already been shown to capture disease-related alterations and to be associated with clinical severity [7]. Recent consensus recommendations also support combining prescribed gait assessment with prolonged monitoring of walking and turning in daily life [5].

Within this context, the Mobilise-D project focused on the use of wearable sensors to obtain digital mobility measures in real-world conditions. The project included the development and validation of algorithms for gait detection and gait-parameter estimation using a single inertial sensor positioned on the lower back [8]. These methods were tested in healthy individuals and in several clinical populations with mobility impairment.

The MobGap library implements this processing framework and provides tools for

detecting walking and estimating digital mobility outcomes from lower-back inertial data. The use of a single sensor is particularly suitable for prolonged monitoring because it reduces the burden on the participant compared with multi-sensor configurations.

Moving from controlled testing to free-living monitoring also introduces additional problems. Algorithm performance may change depending on the gait pattern and on the walking condition. Turning, slower walking, or the use of assistive devices may all affect the recorded signals and the resulting estimates. Validation against an appropriate reference system is therefore needed before these measures can be interpreted with confidence [8].

1.4 Aim and objectives of the thesis

MobGap has already been evaluated in healthy individuals and in different clinical populations characterised by mobility impairment [8]. People with ataxia, however, were not included in the original validation cohorts. Since ataxic gait is variable and often unstable, the performance of the same approach in this population cannot be assumed.

The main aim of this thesis was therefore to evaluate MobGap performance in people with ataxia using a single lower-back inertial sensor. MobGap estimates were compared with measurements obtained from the validated INDIP multi-sensor reference system during standardised and unstructured walking tests.

The first part of the analysis focused on stride detection. For strides detected by both systems, the accuracy of stride duration, stride length, and walking speed was then evaluated.

Performance was also examined under conditions that could affect the single-sensor estimates. In particular, the analysis considered rollator use and walking condition, with straight and turning strides evaluated separately.

Sensor orientation was also investigated after poor stride-detection performance was observed in one participant. An additional gravity-based reorientation was applied to the lower-back signals and MobGap performance was evaluated again.

Finally, when 7-day recordings were available, the same pipeline was applied to free-living data. These recordings were used to compare gait during daily life with gait measured during the clinical tests and to investigate how turning affected the amount of data retained for analysis.

1.4.1 Thesis outline

The thesis is organised as follows:

- **Chapter 2 – Background and state of the art:** provides the background on physiological and ataxic gait, reviews the main technologies used for quantitative gait analysis, and discusses wearable and free-living gait assessment. The chapter concludes with the research gap addressed in this thesis.
- **Chapter 3 – Materials:** describes the INDIP reference system and the Axivity AX6 sensor. It also presents the participants, the experimental protocol, and the 7-day data collection.
- **Chapter 4 – Data Processing and Methods:** describes data preparation and processing, the stride-matching procedure, and the evaluation of MobGap performance. The analyses according to rollator use, walking condition, sensor reorientation, and free-living recordings are also presented.
- **Chapter 5 – Results:** reports stride-detection performance and gait-parameter estimation results. Participant-specific results, rollator use, straight and turning walking, sensor reorientation, and the 7-day recordings are presented separately.
- **Chapter 6 – Discussion:** discusses the main results in relation to previous studies, with particular attention to rollator use, turning, sensor orientation, and the interpretation of free-living gait measurements.
- **Chapter 7 – Conclusion:** summarises the main findings, discusses the main limitations of the study, and presents possible directions for future work.

Chapter 2

Background and state of the art

This chapter introduces the main concepts needed for the present study. It first describes physiological and ataxic gait, followed by the main technologies used for quantitative gait analysis. Particular attention is then given to wearable sensors and free-living assessment, before discussing the limitations of the available literature and the research gap addressed in this thesis.

2.1 Fundamentals of gait analysis

Gait analysis is the quantitative study of human walking. It can be used to describe physiological gait, identify alterations associated with pathological conditions, monitor changes over time, and assess the effects of therapeutic or rehabilitation interventions [9, 10, 11]. Depending on the purpose of the assessment, different aspects of walking can be considered, including spatio-temporal parameters, joint kinematics, kinetics, muscle activation, and energy expenditure.

Walking is one of the main forms of human locomotion and is essential for independent mobility. Although it is mostly automatic during everyday activities, it requires the coordinated action of the musculoskeletal and nervous systems together with continuous sensory feedback. Alterations in walking can therefore reflect changes in motor control or in the general functional status of a person.

Among the variables commonly used in gait analysis, *spatio-temporal gait parameters* provide a direct description of how walking is organised in space and time. They include measures related to progression, rhythm, and timing. Walking speed is one of the most frequently reported parameters and has also been associated with clinically relevant outcomes such as disability, hospitalization, and survival [12].

2.1.1 Physiological gait

Physiological gait is a cyclic movement produced by the alternating action of the lower limbs. During walking, the body has to progress forward while maintaining postural stability, absorbing the impact generated at foot–ground contact, and limiting unnecessary energy expenditure [10].

These functions involve the lower limbs, pelvis, and trunk and require continuous control by the nervous system. Spinal neuronal networks contribute to the generation of the basic locomotor rhythm. Supraspinal structures and sensory information then allow this pattern to be adapted, for example when walking starts or stops, speed changes, or the surrounding environment requires a different motor response [13, 14].

During steady-state walking, such as straight walking at an approximately constant speed, the movement can be considered quasi-periodic. Consecutive cycles are similar, although a certain amount of stride-to-stride variation is also present in physiological gait. Because of this repeated pattern, walking can be divided into individual cycles and described through specific gait events and spatio-temporal parameters [10, 11].

The basic unit of walking is the *gait cycle*, commonly referred to as a *stride*. A stride is defined as the interval between two consecutive initial contacts of the same foot. A *step*, on the other hand, extends from the initial contact of one foot to the following initial contact of the opposite foot. A complete stride therefore contains two consecutive steps, as illustrated in Figure 3.4.

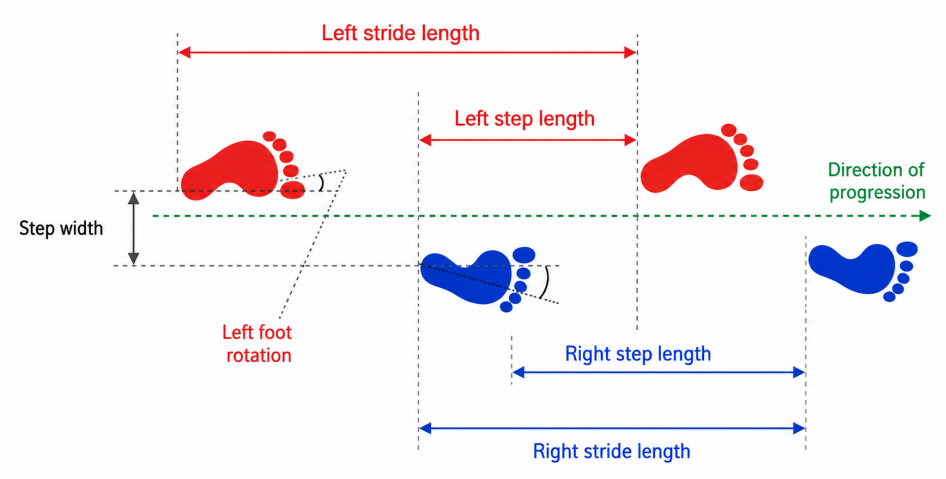


Figure 2.1: Schematic representation of step and stride during walking.

For each lower limb, the gait cycle is divided into a *stance phase* and a *swing phase*. The stance phase starts at initial contact and ends when the foot leaves the

ground. During physiological walking it represents approximately 60% of the gait cycle. During this part of the cycle, the limb accepts body weight, supports the body, and contributes to progression. The swing phase accounts for the remaining approximately 40% and corresponds to the advancement of the limb before the next initial contact [10, 11].

The stance phase can be further divided into initial contact, loading response, mid stance, terminal stance, and pre-swing. Initial swing, mid swing, and terminal swing form the swing phase. Two periods of double support also occur during a normal gait cycle, when both feet are simultaneously in contact with the ground. Their duration becomes shorter as walking speed increases and they disappear during running [10].

Once gait events have been identified, different *spatio-temporal gait parameters* can be calculated. Temporal parameters describe the timing and rhythm of walking and include step duration, stride duration, stance and swing duration, double-support duration, and cadence. Spatial parameters describe progression and foot placement and include step length, stride length, and step width [11]. The present work focuses mainly on *stride duration*, *stride length*, and *walking speed*.

- **Stride duration** is the time between two consecutive initial contacts of the same foot. It corresponds to the duration of one complete gait cycle and describes the temporal organisation of walking.

- **Stride length** is the distance travelled in the direction of progression between two consecutive initial contacts of the same foot. It is the distance covered during a complete gait cycle and depends on the movement of the lower limbs, balance control, and the walking strategy adopted by the individual.

- **Walking speed** describes how rapidly the body progresses forward. It depends on both the temporal and spatial characteristics of gait and, at stride level, can be calculated as

$$v = \frac{L_{\text{stride}}}{T_{\text{stride}}}, \tag{2.1}$$

  where v is walking speed, L_{stride} is stride length, and T_{stride} is stride duration. Changes in walking speed can therefore result from changes in stride length, stride duration, or both.

These three parameters describe different aspects of walking and were selected as the main gait outcomes for the performance evaluation carried out in this thesis.

2.1.2 Ataxic gait

Ataxic gait is characterised mainly by impaired dynamic balance and reduced coordination during progression. Consecutive strides are generally less regular than in physiological walking, with larger variations in both spatial and temporal gait characteristics [4, 5].

From a clinical point of view, people with ataxia may show an unstable or staggering gait, a wider base of support, and irregular foot placement. Maintaining a consistent walking direction can also be difficult. One of the most characteristic features is the increased variability between consecutive strides, which can affect parameters such as step length, stride length, step width, and stride timing [4, 5].

Differences can also be observed in average spatio-temporal parameters. People with ataxia often walk more slowly and with shorter steps, a wider base of support, and longer periods of double support. Some of these changes are not specific to ataxia and may represent compensatory strategies used to increase stability. Increased spatial and temporal variability, instead, is more directly linked to the loss of coordination that characterises ataxic gait [5].

The irregularity of the gait pattern is relevant when automated methods are used for quantitative analysis. Several gait-analysis algorithms rely, at least partly, on recurring patterns in consecutive gait cycles. In ataxia, larger variations in stride timing, foot placement, and trunk motion can make these patterns less repeatable. Gait events may therefore be more difficult to detect and spatio-temporal parameters more difficult to estimate automatically.

The walking pattern can become even less regular when the task is more demanding. Turning and changing direction require continuous adjustments of balance, body orientation, and foot placement. The same applies when a person has to adapt to obstacles or to the surrounding environment. For this reason, impairments that are not very evident during steady straight walking may become more visible in more complex walking conditions.

Gait variability is also clinically relevant. In studies based on wearable inertial sensors, spatial variability measures have been able to distinguish individuals with degenerative cerebellar ataxia from healthy controls and have shown associations with clinical measures of disease severity [7]. Quantitative gait and balance measures, including variability-related outcomes, have consequently been identified as promising digital measures for the assessment and monitoring of ataxia [5].

2.2 Technologies for gait analysis

Different measurement technologies can be used to obtain quantitative information about gait. Some systems focus mainly on body movement, while others measure forces, foot–ground interaction, or acceleration and angular velocity. The choice depends on the type of variable that needs to be measured, the required accuracy, and the environment in which the assessment is performed [9, 15].

Traditional laboratory systems, such as optoelectronic motion capture and force platforms, allow detailed biomechanical measurements under controlled conditions. Wearable devices, including pressure insoles and inertial sensors, provide less detailed information in some respects but are easier to use outside the laboratory and during longer recordings. This difference becomes particularly important when gait is studied not only during short clinical tests but also during daily activities.

2.2.1 Optoelectronic Motion Capture System

Optoelectronic motion capture systems based on stereophotogrammetry are widely used as reference systems for three-dimensional human movement analysis [9, 16]. They usually consist of several cameras placed around a calibrated measurement volume and a set of retroreflective markers attached to selected anatomical landmarks.

Each camera records the two-dimensional position of the markers visible within its field of view. When the same marker is seen by more than one calibrated camera, its three-dimensional position can be reconstructed by triangulation. The resulting marker trajectories can then be combined with biomechanical models to estimate segment positions, joint angles, velocities, and accelerations. Figure 3.4 shows a typical laboratory configuration.

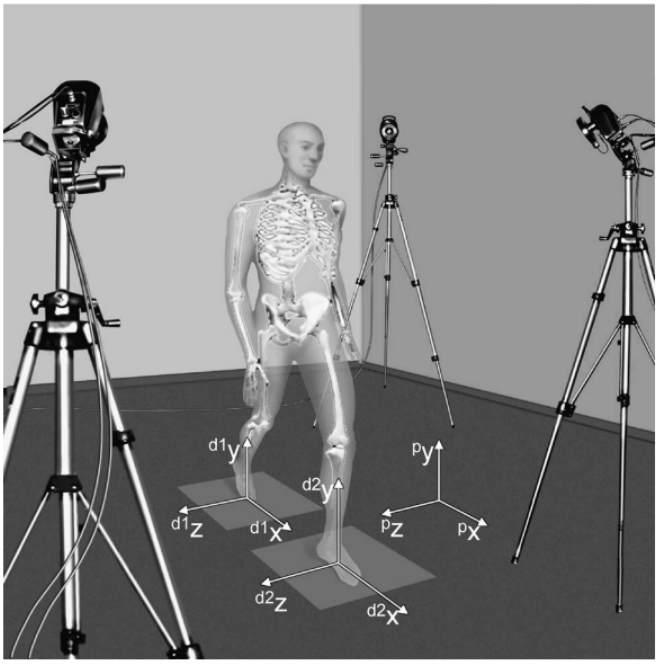


Figure 2.2: Human movement analysis laboratory showing the main measurement systems and their reference frames. Reproduced from Cappozzo et al. [16].

Their main advantage is the high spatial and temporal accuracy that can be achieved under controlled conditions. This makes optoelectronic systems suitable for detailed biomechanical analysis and for the validation of other movement-analysis technologies. They can also be combined with force platforms and electromyography when both kinematic and kinetic information is required [16].

There are, however, several practical constraints. The cameras have to be calibrated, markers must be positioned carefully, and data collection usually requires trained personnel. Marker trajectories can also be affected by occlusion and soft-tissue artefacts. More importantly for real-world gait assessment, the participant has to remain inside the calibrated capture volume. Only a limited walking distance can therefore be recorded. This makes optoelectronic motion capture very useful for laboratory analysis but impractical for prolonged monitoring of habitual walking.

2.2.2 Force platform

Force platforms measure the forces generated between the foot and the ground. They are generally installed in the laboratory floor and include force and moment transducers that measure the three components of the ground reaction force (GRF), together with the corresponding moments. An example is shown in Figure 3.4.

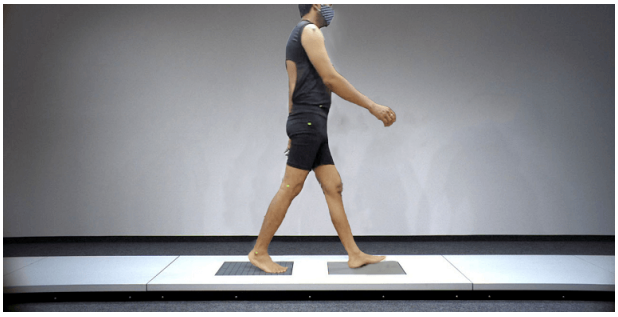


Figure 2.3: Example of a force platform used for the measurement of ground reaction forces during gait analysis. Reproduced from Auptimo [17].

During walking, the GRF represents the external force applied by the ground to the body during foot contact. Its vertical component mainly reflects body-weight support. The anteroposterior component is related to braking and propulsion, while the mediolateral component gives information about lateral control. The measured forces and moments can also be used to calculate the centre of pressure (CoP), which indicates the point of application of the resultant ground reaction force.

Force-platform data are often analysed together with motion-capture measurements. When body-segment kinematics and external forces are both available, inverse-dynamics methods can be used to estimate joint moments and powers [9]. This allows a more detailed analysis of the mechanisms involved in walking.

Force platforms are also useful for identifying gait events because the beginning and end of foot–ground contact can be measured accurately. The main limitation is that the measurement is restricted to the physical area of the platform. The participant has to step correctly on it, and only a limited number of consecutive steps can usually be recorded. For this reason, force platforms are mainly used for laboratory measurements rather than for long or unconstrained walking tasks.

2.2.3 Pressure insoles

Instrumented pressure insoles provide a wearable alternative for measuring foot–ground interaction. They consist of thin and flexible insoles containing a number of pressure- or force-sensitive elements distributed over the plantar surface. Different technologies can be used, including resistive, capacitive, piezoresistive, and piezoelectric sensors. The INDIP system used in this thesis includes instrumented pressure insoles, whose sensor distribution is shown in Figure 3.4.

The main difference compared with a force platform is that the insole moves with the participant. Foot contact can therefore be measured over many consecutive strides and is not restricted to a small area of the laboratory. The distribution of plantar loading over time can be used to study pressure patterns, load transfer,

CoP progression, and the timing of the different phases of the gait cycle.

Pressure signals can also be used to detect gait events. The activation of plantar sensors indicates that the foot has reached the ground, whereas their deactivation can be used to identify the end of stance. Initial and final contact can therefore be detected directly from the pressure pattern, from which parameters such as stance duration, swing duration, step duration, and stride duration can be calculated [18].

Their wearable configuration is useful when reliable information about foot contact is required outside the restricted measurement area of a force platform. Measurement quality still depends on the type of sensor, calibration, footwear, and the position of the insole inside the shoe. Resistive sensors, for example, can show hysteresis and drift, and the measured pressure distribution may change with shoe fit or small changes in insole placement. Validated systems can nevertheless provide reliable gait-event information during both structured tests and less controlled walking tasks [18, 19].

2.2.4 MIMU

The development of Micro-Electro-Mechanical Systems (MEMS) has made inertial sensors small and lightweight enough to be worn directly on the body. A Magneto-Inertial Measurement Unit (MIMU) generally includes a tri-axial accelerometer, a tri-axial gyroscope, and a tri-axial magnetometer, for a total of nine sensing axes. Devices containing only an accelerometer and a gyroscope are generally referred to as Inertial Measurement Units (IMUs). The main sensing components of a MIMU are illustrated in Figure 3.4.

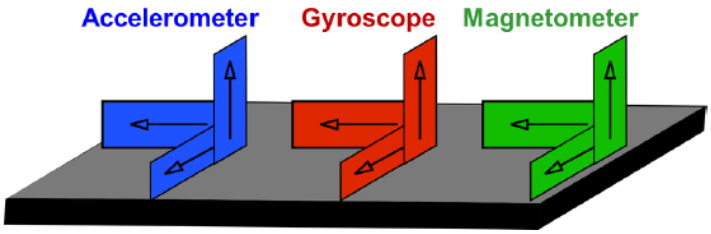


Figure 2.4: Main sensing components of a Magneto-Inertial Measurement Unit (MIMU), combining a tri-axial accelerometer, gyroscope, and magnetometer.

Each sensor measures a different physical quantity. Accelerometers measure specific force, gyroscopes measure angular velocity, and magnetometers measure the local magnetic field. Depending on the application, these signals can be processed separately or combined through sensor-fusion methods to estimate movement and orientation of the body segment on which the device is placed [20].

Inertial sensors do not require cameras, external emitters, or a predefined capture volume. They can be attached to body segments such as the feet, shanks, trunk, or lower back, and data can be collected over much longer periods than with most laboratory systems. These characteristics have made them particularly useful for wearable gait analysis and for measurements performed outside conventional motion-analysis laboratories [15].

Their measurements are not free from error. Sensor bias, noise, scale-factor errors, axis misalignment, and integration drift can all affect the signals. Another important aspect is sensor orientation. Raw inertial measurements are expressed in the local coordinate system of the device, so the relationship between sensor axes and anatomical directions depends on how the sensor has been positioned. This becomes relevant whenever one specific component of acceleration or angular velocity is interpreted as vertical, mediolateral, or anteroposterior motion.

The operating principles of the three sensing elements are described below.

Accelerometer

An accelerometer measures the *specific force* acting along its sensitive axes. Wearable accelerometers are usually tri-axial, so measurements are collected along three orthogonal directions.

A MEMS accelerometer can be described, in simplified mechanical terms, as a mass–spring–damper system. A microscopic proof mass is suspended inside the sensor by elastic structures. When the sensor accelerates, the inertia of the proof mass causes a small displacement relative to the surrounding frame. The sensor detects this displacement and converts it into an electrical signal related to acceleration [21]. Figure 3.4 shows a simplified representation.

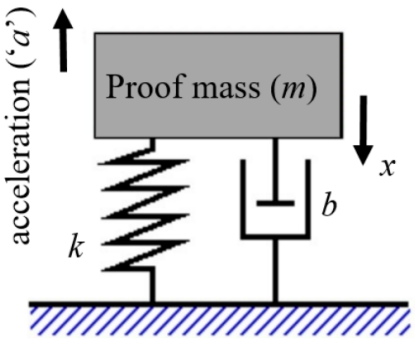


Figure 2.5: Mass–spring–damper representation of a MEMS accelerometer. An applied acceleration produces a relative displacement of the proof mass with respect to the sensor frame. Reproduced from Mohammed et al. [21].

The measurement can be represented in simplified form as

$$\mathbf{f} = \mathbf{a} - \mathbf{g}, \tag{2.2}$$

where $\mathbf{f}$ is the measured specific force, $\mathbf{a}$ is the translational acceleration of the sensor, and $\mathbf{g}$ is the gravitational acceleration vector.

Gravity is therefore always present in accelerometer measurements. When the device is stationary, translational acceleration is zero and the values measured along the three sensor axes depend on how gravity is projected onto them. Static or quasi-static measurements can consequently be used to obtain information about sensor inclination. During movement, the recorded acceleration contains both dynamic and gravitational components, and a different orientation of the device changes the distribution of gravity among the three axes.

During walking, repeated steps generate characteristic patterns in trunk and limb accelerations. These patterns can be used to identify walking periods, detect gait events, study trunk dynamics, and estimate spatio-temporal gait parameters.

Gyroscope

A gyroscope measures angular velocity around its sensing axes, generally expressed in degrees per second or radians per second. A tri-axial gyroscope therefore provides the three components of the angular velocity vector.

Most wearable MEMS gyroscopes operate using the Coriolis effect. A microscopic proof mass is kept in oscillation along a predefined direction. If the sensor rotates while the mass is moving, a Coriolis force acts in a direction perpendicular to the original motion. In simplified form,

$$\mathbf{F}_C = 2m(\mathbf{v} \times \boldsymbol{\omega}), \tag{2.3}$$

where m is the proof mass, $\mathbf{v}$ is its oscillatory velocity, and $\boldsymbol{\omega}$ is the angular velocity of the sensor. The displacement generated by this force is detected by the sensing structure and converted into an electrical output proportional to angular velocity.

Gyroscopes are particularly useful in gait analysis when rotational movements have to be measured. Trunk rotation and changes in walking direction, including turns, produce clear changes in angular velocity. Unlike accelerometers, gyroscope measurements are not directly affected by gravity. Problems arise when angular velocity is integrated over time to obtain orientation, since even a small constant bias can accumulate and produce an increasing orientation error known as *drift*.

A simplified measurement model can be written as

$$\boldsymbol{\omega}_m(t) = \boldsymbol{\omega}(t) + \mathbf{b}(t) + \mathbf{n}(t), \tag{2.4}$$

where $\boldsymbol{\omega}_m$ is the measured angular velocity, $\boldsymbol{\omega}$ is the true angular velocity, $\mathbf{b}$ is the sensor bias, and $\mathbf{n}$ represents measurement noise. For orientation estimation, gyroscope data are therefore often combined with accelerometer measurements and, when available, magnetometer information.

Magnetometer

A magnetometer measures the magnitude and direction of the local magnetic field along three orthogonal axes. In a MIMU, the Earth's magnetic field can provide an external directional reference, especially for heading or yaw, which cannot be determined from gravity alone [20].

Many MEMS magnetometers use electromagnetic sensing principles such as the Hall effect. When electrical charges moving through a conductive material are exposed to a magnetic field, the Lorentz force causes a transverse displacement of the charges. This generates a voltage that is related to the magnetic-field component acting on the sensor.

Magnetometer measurements can therefore complement the information obtained from accelerometers and gyroscopes. Their main limitation is the sensitivity to magnetic disturbances. Metallic structures, ferromagnetic objects, electrical equipment, and other nearby sources can change both the magnitude and direction of the magnetic field measured by the device.

These disturbances are commonly divided into *hard-iron effects*, which mainly produce an offset, and *soft-iron effects*, which distort the magnitude and direction of the measured field. Calibration is usually required when magnetometer signals are used for orientation estimation [22].

Accelerometers, gyroscopes, and magnetometers therefore provide different information and are affected by different sources of error. Their combination makes it possible to obtain a more complete description of body movement and forms the basis of magneto-inertial sensing in wearable movement analysis.

2.3 Free-living gait assessment

Clinical and laboratory gait tests are performed in controlled and repeatable conditions. These measurements are useful, but they represent only a limited sample of how a person walks. Everyday walking is usually less regular and includes different speeds, walking-bout durations, changes in direction, stops, and interactions with the environment [8, 23].

Wearable inertial sensors make it possible to collect data over much longer periods without restricting the participant to a laboratory space. Movement can be recorded while the person carries out normal daily activities, and digital mobility outcomes can then be extracted from these data [5, 8].

The distinction between controlled and real-world measurements is particularly relevant when gait is used to describe functional mobility. A person's ability to perform a walking task under standardized conditions and the way that person actually moves during daily life are related, but they are not the same concept [23, 24].

2.3.1 Gait capacity vs gait performance

The International Classification of Functioning, Disability and Health (ICF) distinguishes between *capacity* and *performance* [24]. Capacity refers to an individual's ability to perform a task or action under standardized environmental conditions. In gait assessment, it is usually measured through clinical or laboratory tests in which the instructions, environment, and measurement procedure are controlled.

Performance describes what the person actually does in the current environment [24]. Daily mobility depends not only on motor ability but also on the physical environment, habits, motivation, and the activities that have to be performed. Two individuals with similar results during a standardized walking test may therefore show quite different mobility patterns during everyday life [23, 24].

Giannouli et al. investigated this difference in older adults by comparing laboratory-based mobility capacity with real-life mobility performance [23]. The association between the two was only moderate. Laboratory measures explained approximately 5–21

Free-living monitoring provides a way to observe the performance component more directly. Instead of analysing only a few predefined walking trials, wearable devices can collect information from many walking episodes occurring naturally throughout the day [8]. Clinical and free-living assessments can then provide different views of the same person's mobility rather than being considered interchangeable measurements.

2.3.2 Relevance of free-living gait assessment in ataxia

This distinction is particularly relevant in cerebellar ataxia because gait and balance problems are among the major manifestations of the disease [5]. Quantitative digital measures have been proposed for the description of disease severity and for monitoring progression in natural-history studies and clinical trials [5].

Standardized clinical tests remain important, but they contain only a small number of walking tasks performed for a limited time. Wearable sensors allow gait to be measured for longer periods in the person's usual environment [5]. Daily-life recordings include situations that are difficult to reproduce systematically in the clinic, such as frequent direction changes, short walking episodes, and natural variation in walking speed [5, 7].

Ilg et al. compared people with degenerative cerebellar ataxia and healthy controls during laboratory walking, supervised free walking, and real-life walking using wearable inertial sensors [7]. Spatial gait-variability measures were able to identify ataxic gait in all three conditions. During real-life walking, lateral step deviation combined with a compound measure of spatial variability distinguished participants with ataxia from healthy controls with an accuracy of 0.86 [7]. The same measures were strongly associated with clinical ataxia severity, with a correlation of $\rho = 0.76$. The largest effect sizes for differences in gait severity were found during real-life walking [7].

The Ataxia Global Initiative has also highlighted digital gait measures as potentially useful outcomes for both standardized and everyday-life assessment [5]. Recordings performed in habitual environments can provide information about walking behaviour over a longer period and under conditions that are closer to the person's normal daily activities.

At the same time, free-living recordings are more difficult to analyse. Walking episodes differ in duration and speed, and the same algorithm may not perform equally well in all of them [8]. In the Mobilise-D validation study, lower performance was observed for several gait outcomes during shorter walking bouts and at slower walking speeds. Validation therefore needs to include conditions that resemble those in which the method will eventually be used [8].

2.4 Current limitations and research gap

Inertial sensors have already been used to study gait in people with ataxia, both during standardised walking tests and in daily life. The available studies, however, have addressed different questions and have used different sensor configurations.

During standardised assessments, gait characteristics have been quantified using wearable inertial sensors. Matsushima et al. used a single triaxial accelerometer positioned on the back during repeated 10-m walking trials in people with spinocerebellar ataxia or multiple-system atrophy [25]. They analysed gait velocity, cadence, step length, regularity, symmetry, and body sway. Shah et al. instead used a multi-sensor inertial setup during a standardised 2-min walking test and showed that gait variability was associated with disease severity in spinocerebellar ataxia [26].

These studies show that inertial sensors can capture relevant characteristics of ataxic gait. In particular, the work by Matsushima et al. shows that useful gait information can also be obtained from a single sensor placed on the trunk. However, these measurements were collected during short and prescribed walking tasks. The studies were also not designed as a technical validation of a single-sensor gait-analysis pipeline against an independent reference system.

Wearable sensors have also been used to study gait in people with ataxia outside standardised laboratory conditions. Ilg et al. compared laboratory walking, supervised free walking, and real-life walking in people with degenerative cerebellar ataxia [7]. Spatial gait variability measured in daily life was strongly related to clinical ataxia severity. More recently, Shah et al. compared a prescribed clinical walking test with one week of daily-life monitoring and found that 13 of the 17 analysed gait measures differed between the two environments [27].

These real-world studies provide important information about habitual gait in ataxia, but both used a three-sensor configuration, with one sensor on each foot and one on the lower back [7, 27]. Their main focus was the characterisation of gait and its relationship with disease severity rather than the technical validation of gait parameters obtained from a single lower-back sensor.

A single-sensor approach would be simpler for prolonged monitoring. The Mobilise-D project specifically investigated this configuration and validated algorithms based on one lower-back inertial sensor in healthy older adults and in several clinical populations, including Parkinson's disease, multiple sclerosis, proximal femoral fracture, chronic obstructive pulmonary disease, and congestive heart failure [8]. People with ataxia, however, were not included in these validation cohorts.

This leaves a specific methodological gap. Although inertial sensing has already been applied to ataxic gait, the MobGap single lower-back sensor pipeline has not been validated in this population. It is therefore not known whether this configuration can reliably detect strides and estimate stride duration, stride length, and walking speed in people with ataxia.

This question is particularly relevant because ataxic gait is highly variable and because walking conditions such as turning and the use of walking aids may further modify the signal measured at the lower back. Evaluating MobGap against an independent reference system under these conditions is therefore the main focus of the present thesis.

Chapter 3

Materials

This chapter presents the materials and dataset used in the present study. The INDIP reference system and the Axivity AX6 wearable sensor are first described, followed by an overview of the enrolled participants, the experimental protocol, and the available 7-day recordings.

3.1 INDIP reference system

The reference system used in this study was the INDIP system (*INertial module with DIstance sensors and Pressure insoles*). The system was developed by the University of Sassari in collaboration with other research institutions involved in the Mobilise-D project [19, 29, 30]. It was designed to provide wearable reference measurements for gait assessment under conditions that are less controlled than those typically investigated in a motion analysis laboratory, including complex structured walking tests, simulated daily-life activities, and recordings performed in real-world environments.

The INDIP system was initially evaluated against stereophotogrammetry during laboratory experiments and was subsequently tested in a multicentre validation study involving healthy participants and people with different conditions affecting mobility. High agreement with stereophotogrammetric measurements was reported across different walking tasks and participant groups [19, 29]. These results support its use as a wearable reference system for the estimation of spatial and temporal gait parameters when conventional laboratory systems cannot be used.

The INDIP configuration is shown in Figure 3.4. It consists of two plantar pressure insoles (PIs), three magneto-inertial measurement units (MIMUs), and two infrared Time-of-Flight distance sensors (DSs). The pressure insoles provide information about foot–ground contact. Two MIMUs are positioned on the instep of the feet, while the third is attached to the lower back. The distance sensors

are placed on the lower legs and measure changes in the relative distance between them during walking [19].

The MIMUs and pressure insoles acquire data at 100 Hz, while the distance sensors operate at 50 Hz, with their measurement range set to 0.2 m [19, 29].

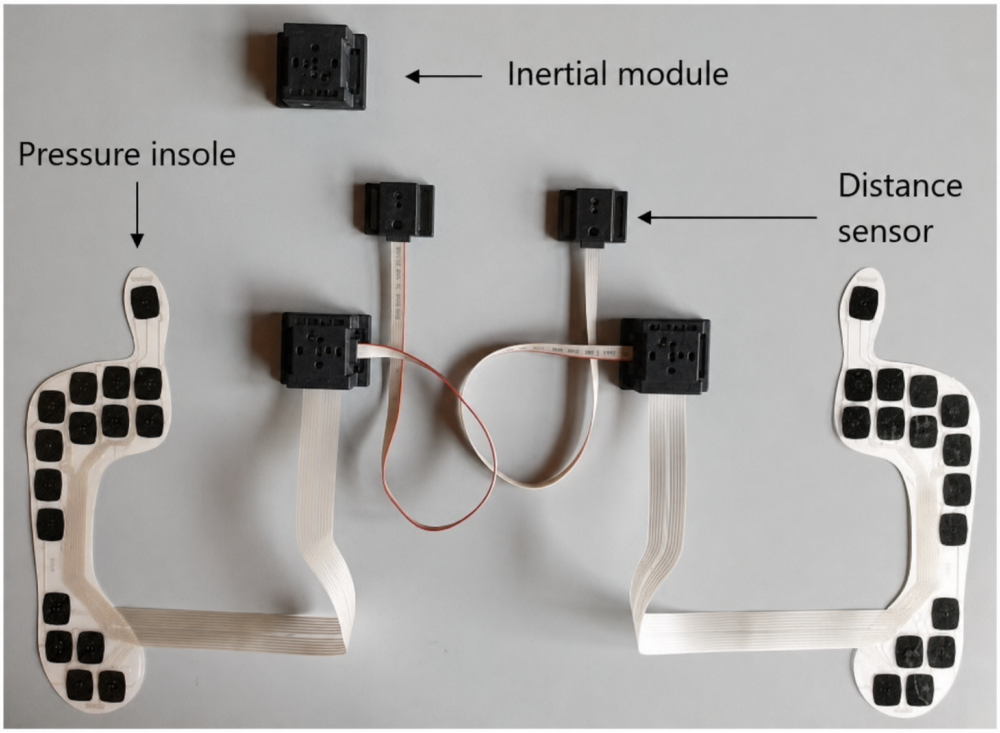


Figure 3.1: Complete INDIP configuration and positioning of the pressure insoles, foot-mounted MIMUs, lower-back MIMU, and distance sensors. Adapted from Salis et al. [19].

During sensor placement, the sensing axes were oriented as consistently as possible with the anatomical directions. In particular, the lower-back sensor was positioned so that its axes were approximately aligned with the vertical, medio-lateral, and anteroposterior directions of the body. The conventional orientation adopted for the sensors is shown in Figure 3.4.

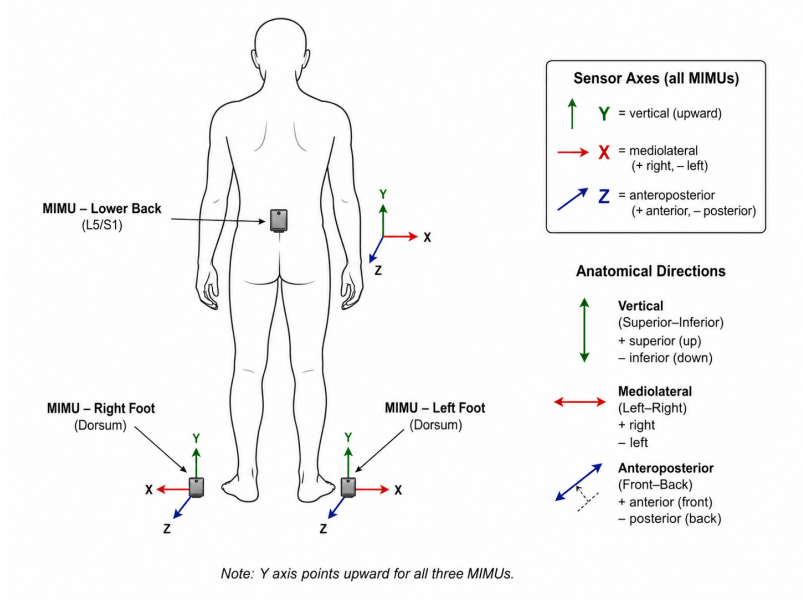


Figure 3.2: Conventional positioning and orientation of the INDIP sensors with respect to the anatomical axes.

The main components of the INDIP system are described in the following sections.

3.1.1 INDIP MIMUs

The INDIP system includes three MIMUs, each sampled at 100 Hz. Each unit contains a three-axis accelerometer, a three-axis gyroscope, and a three-axis magnetometer, providing three-dimensional measurements of acceleration, angular velocity, and magnetic field [19, 29].

The accelerometer and gyroscope full-scale ranges were set to ± 16 g and $\pm 2000°/s$, respectively, while the magnetometer had a measurement range of ± 50 Gauss [19, 29].

The MIMU main board includes a 32-bit ARM Cortex-M4 microcontroller, onboard memory, Bluetooth Low Energy communication, and connectors for external sensing peripherals. It also supplies power to the pressure insole and distance sensor connected to it and manages data acquisition and storage [19].

Two MIMUs were fixed to the instep of the shoes using dedicated clips, whereas the third was attached to the lower back using an elastic belt. The foot-mounted MIMUs were used to estimate foot orientation, velocity, and displacement, while the lower-back MIMU provided information for activity recognition and turning detection. Before each acquisition, a short static recording was performed to estimate gyroscope bias and check the correct operation of the inertial sensors [19].

3.1.2 INDIP pressure insoles

The INDIP system includes two plantar pressure insoles, one for each foot. Each insole contains 16 force-sensitive resistor elements, with an area of approximately 310 mm^2 per sensing element [18]. Nine sensing elements cover the forefoot region, two the midfoot, and five the rearfoot, as shown in Figure 3.4.

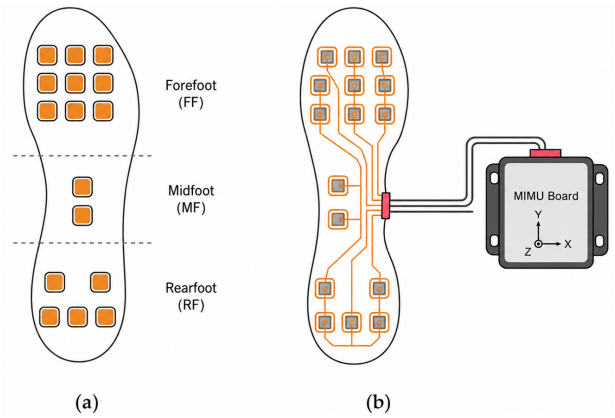


Figure 3.3: Distribution of the 16 force-sensitive resistor elements in the INDIP pressure insole. The sensing elements cover the forefoot, midfoot, and rearfoot regions. Adapted from Salis et al. [18].

The complete insole has an overall thickness of approximately 240 μm and is covered by a polyester layer, making it thin and flexible enough to be inserted inside the participant's shoe [19]. In the configuration used in this study, pressure signals were sampled at 100 Hz.

Each pressure insole was connected by a thin cable to the MIMU positioned on the corresponding foot, which supplied power to the insole and managed data acquisition and storage.

The pressure signals were used to identify initial and final contacts between the feet and the ground. Gait-event detection was based on the activation and deactivation of neighbouring groups of sensing elements rather than on a single sensor, improving robustness to noise and local variations in plantar loading. When validated against force platforms, the method showed average timing errors of approximately 20 ms for initial contacts and 10 ms for final contacts [18].

3.1.3 INDIP distance sensors

The INDIP system includes two infrared Time-of-Flight distance sensors. Each device combines an infrared emitter, a range sensor, and an ambient light sensor.

During the INDIP acquisitions, the measurement range was set to 0.2 m and the sampling frequency to 50 Hz [19].

Time-of-Flight sensors estimate the distance from a target using the infrared signal emitted by the device and subsequently reflected back towards the sensor. In the device used within the INDIP system, distance estimation is based on the phase difference between the emitted and reflected signals. The operating principle is illustrated in Figure 3.4.

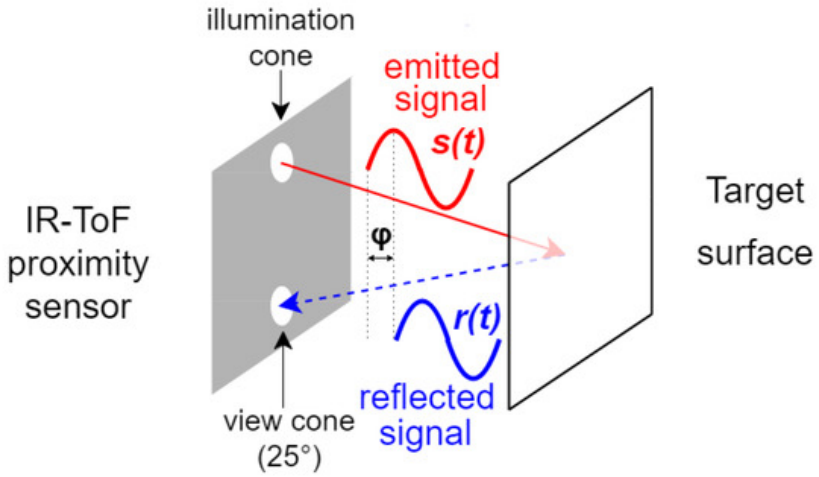


Figure 3.4: Operating principle of the infrared Time-of-Flight proximity sensor. The distance from the reflecting target is estimated by measuring the phase shift between the emitted and reflected signals. Reproduced from Bertuletti et al. [31].

The two distance sensors were positioned asymmetrically on the lower legs to reduce mutual infrared interference. One sensor was placed just above the left ankle, while the other was positioned approximately 3 cm higher on the right leg. Both were oriented medially towards the contralateral lower limb and connected by cable to the MIMU of the corresponding foot [19].

During walking, the measured distance changes according to the alternating movement of the lower limbs. These signals were used as an additional source of information for stride detection and to identify possible missing or incorrectly detected strides.

The technology was previously characterised using the D-MuSe wearable platform, which combined a MIMU with an infrared Time-of-Flight sensor. For distances up to 200 mm and incidence angles within approximately ±30°, a mean absolute percentage error of about 2.5under static conditions and up to 10.2[31].

3.2 Axivity sensor

The wearable sensor used in this study was the Axivity AX6 (Axivity Ltd., Newcastle upon Tyne, UK). The AX6 is a compact inertial data logger designed for continuous movement monitoring. It includes a three-axis accelerometer and a three-axis gyroscope, providing six-axis measurements of linear acceleration and angular velocity. The two sensors are based on MEMS technology, and the acquired signals are stored in their raw form in the internal flash memory [32].

Figure 3.5 shows the Axivity AX6 sensor used in this study.



Figure 3.5: Axivity AX6 wearable inertial sensor used in this study.

The accelerometer measurement range can be configured between ± 2 g and ± 16 g, while the gyroscope range can be selected between $\pm 125°/s$ and $\pm 2000°/s$. Both sensors have a 16-bit resolution. The accelerometer sampling frequency is also configurable, ranging from 12.5 to 1600 Hz [32]. In the present study, the AX6 was configured to acquire both acceleration and angular velocity at 100 Hz.

The device has dimensions of approximately $23 \times 32.5 \times 8.9$ mm and a mass of only 11 g. It includes 1024 MB of non-volatile flash memory and provides more than 7 days of battery life when accelerometer and gyroscope signals are recorded at 100 Hz [32]. Its small size, low weight, internal memory, and battery autonomy make it suitable both for standardized clinical walking tests and for prolonged monitoring in daily-life conditions. The AX6 used in this study was positioned on the lower back at the level of L5.

The acquired raw acceleration and angular-velocity signals were stored in the internal memory using the CWA binary format. The structure and processing of these files are described in Section 4.5.1.

3.3 Overview of data collection

Data collection was conducted at the Royal Hallamshire Hospital in Sheffield. Five participants with ataxia were enrolled in the study.

Two self-reported health measures were also available: the *SF-12 Physical Component Summary (PCS)*, which summarises the physical health component of the 12-Item Short Form Health Survey, and the *EQ-VAS*, which provides a self-rated assessment of overall health on a scale from 0 (worst imaginable health) to 100 (best imaginable health). For both measures, higher scores indicate a better perceived health status.

Table 3.1 summarises the available information for each participant, including participant ID, age, sex, walking aid, health measures, number of available walking tests used for performance evaluation, and availability of the 7-day recording. The number of available tests refers only to the four walking tests included in the performance evaluation, namely the Timed Up and Go, Straight Walk, 6-Minute Walk Test, and Unstructured Walk. The first three protocol tests, which were used for calibration, orientation, and personalisation, are therefore not included in this count. Consequently, a value of 4 indicates that all walking tests used for performance evaluation were available for that participant.

3.4 Experimental protocol

The complete experimental protocol consisted of seven tests. The first three tests were performed for sensor calibration, orientation, and participant-specific personalization and were not included in the performance evaluation. The performance of the MobGap pipeline was assessed exclusively using the four walking tests corresponding to Tests 4–7: the Timed Up and Go, Straight Walk, 6-Minute Walk Test, and Unstructured Walk.

The complete protocol consisted of the following tests:

1. **Test 1: Static Calibration.** This test was performed before positioning the sensors on the participant. It was used to calibrate the sensors and remove potential baseline offsets.

2. **Test 2: Standing Posture.** The participant was instructed to stand as still as possible for approximately 30 seconds. This trial was used for sensor orientation and calibration.

3. **Test 3: Personalization (Pers).** The participant was asked to perform the following sequence of movements:

    - stand in a static position for a few seconds;

Table 3.1: Participant characteristics and data availability.

Participant	ID	Age	Sex	Walking aid	Health Measures		Available tests	7-day recording
					SF-12 PCS	EQ-VAS		
S1	0239	70	Female	No	26.92698	80	3	Yes
S2	807	67	Female	Stick	24.96879	35	1	Yes
S3	192	71	Female	Rollator	26.69774	75	4	No
S4	811	58	Male	No	51.69815	65	4	No
S5	180	55	Female	Rollator	26.42229	50	4	Yes

- lift the right foot, maintain the position for a few seconds, and then return to a balanced double-support stance;
- repeat the same procedure with the left foot;
- repeat a similar sequence with the upper limbs, first lifting the right arm and then the left arm;
- walk along a J-shaped path by moving forward for a short distance, performing a turn, and walking back.

4. **Test 4: Timed Up and Go (TUG).** The participant started from a seated position, stood up, walked for a distance of 3 m, turned around a cone, returned to the chair, and sat down. The test was repeated twice at the participant's self-selected comfortable walking speed.

5. **Test 5: Straight Walk (SW).** The participant walked along a 10-m straight path at a self-selected comfortable speed. The test was repeated twice.

6. **Test 6: 6-Minute Walk Test (6MWT).** The participant was asked to walk continuously back and forth along a 10-m walkway for a total duration of 6 minutes. The turnaround points were marked by cones, resulting in a distance of 20 m for each complete out-and-back cycle.

7. **Test 7: Unstructured Walk (UW).** The participant was asked to walk freely without following a predefined path. In this study, participants walked within the hospital premises for a variable duration.

The schematic layout of the four walking tests included in the performance evaluation is illustrated in Figure 3.6. Tests 1–3 are not shown because they were used only for calibration, orientation, and personalization.

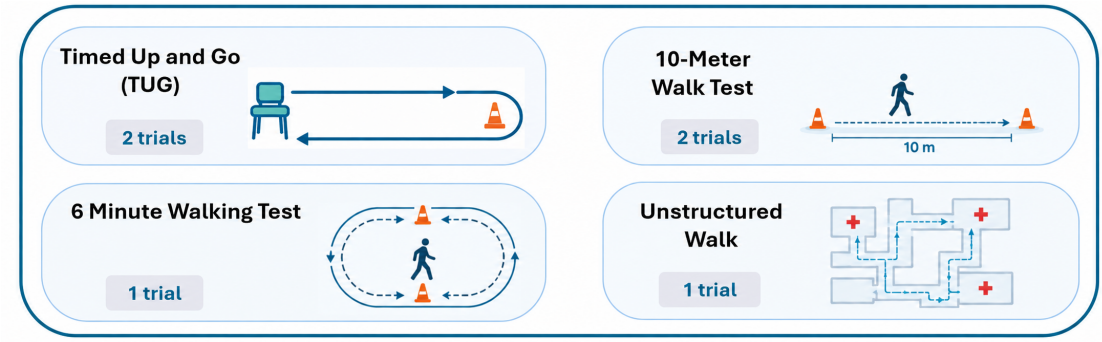


Figure 3.6: Schematic overview of the four walking tests included in the performance evaluation: Timed Up and Go, performed twice; 10-m Straight Walk, performed twice; 6-Minute Walk Test, performed once by continuously walking back and forth along a 10-m walkway; and Unstructured Walk, performed once within the hospital corridors.

The experimental sensor setup used during data collection is shown in Figure 3.7.



Figure 3.7: Experimental sensor setup used during data collection.

3.5 7-day data collection

After completing the clinical tests, participants were asked to wear the Axivity AX6 continuously for 7 consecutive days during their usual daily activities. The sensor was positioned on the lower back at the level of L5 and programmed to start recording at midnight. No INDIP reference system was used during this monitoring period.

Table 3.1 reports the availability of the 7-day recording for each participant.

The processing procedure applied to the continuous recordings is described in Section 4.5.

Chapter 4

Data Processing and Methods

This chapter describes the procedures used to prepare, process, and analyse the data collected during the study. The clinical recordings from Axivity and INDIP were first temporally aligned and organised into corresponding trials. The two systems were then processed independently, and their outputs were matched at stride level to evaluate MobGap performance. Additional analyses were performed according to rollator use, walking condition, and lower-back sensor orientation. Finally, the processing and analysis of the 7-day free-living recordings are described.

4.1 Data preparation

Before applying the INDIP and MobGap processing pipelines, the signals recorded by the two systems were prepared to ensure temporal correspondence across participants, tests, and trials. This included resampling and segmenting the continuous Axivity recordings, refining their temporal alignment with INDIP, and storing the resulting data in a common trial-based structure.

4.1.1 Temporal alignment between INDIP and Axivity

The Axivity device recorded continuous tri-axial acceleration and angular-velocity signals throughout the experimental session. INDIP data, in contrast, were already organised into separate recordings corresponding to individual tests and trials. The continuous Axivity recording therefore had to be segmented and aligned with the corresponding INDIP data before processing.

The complete Axivity accelerometer and gyroscope signals were first resampled to 100 Hz, corresponding to the sampling frequency of the INDIP inertial data.

Resampling was performed before trial segmentation so that all subsequent analyses were carried out at the same sampling frequency.

An initial segmentation was obtained from the `StartDateTime` information associated with each INDIP test and trial. These timestamps were used to identify the corresponding portions of the continuous Axivity recording.

Because Axivity and INDIP operated using independent internal clocks, small temporal offsets could remain after timestamp-based segmentation. A finer alignment was therefore performed by comparing the acceleration recorded by the Axivity sensor with that measured by the INDIP lower-back sensor.

Since the two sensors could have slightly different orientations, acceleration magnitude was used instead of individual sensor axes. For each system, it was calculated as

$$\|\mathbf{a}[n]\| = \sqrt{a_x[n]^2 + a_y[n]^2 + a_z[n]^2}, \tag{4.1}$$

where $a_x[n]$, $a_y[n]$, and $a_z[n]$ are the three acceleration components at sample n.

The remaining temporal offset was estimated by cross-correlating the two acceleration-magnitude signals over a 10-s interval containing a clearly identifiable movement pattern. The lag corresponding to the maximum cross-correlation was taken as the residual sample shift:

$$k_{\text{shift}} = \arg\max_k R_{\text{Axivity,INDIP}}[k], \tag{4.2}$$

where $R_{\text{Axivity,INDIP}}[k]$ is the cross-correlation between the Axivity and INDIP acceleration magnitudes at lag k.

The corresponding temporal offset was

$$\Delta t = \frac{k_{\text{shift}}}{f_s}, \tag{4.3}$$

where $f_s = 100$ Hz. The estimated shift was then applied to the complete Axivity trial, including both accelerometer and gyroscope signals.

Alignment quality was finally checked over the complete trial by superimposing the Axivity and INDIP acceleration magnitudes and verifying that the main movement-related features occurred at the same time. Angular-velocity magnitude was also inspected as an additional check and was calculated as

$$\|\boldsymbol{\omega}[n]\| = \sqrt{\omega_x[n]^2 + \omega_y[n]^2 + \omega_z[n]^2}. \tag{4.4}$$

This final inspection was used to verify that the alignment obtained from the 10-s interval was maintained throughout the trial.

4.1.2 Data organisation

After temporal alignment, the INDIP and Axivity data for each participant were stored in a single MATLAB file named `data.mat`. Recordings were organised hierarchically according to measurement session, test, and trial.

Within each trial, the reference INDIP data were stored in the `SU_INDIP` branch, which retained the complete multi-sensor configuration. The aligned Axivity data were stored in the `SU` branch and contained only the `LowerBack` sensor.

This organisation allowed the two datasets to be processed independently while preserving the correspondence between recordings. The resulting data structure is illustrated in Figure 4.1.

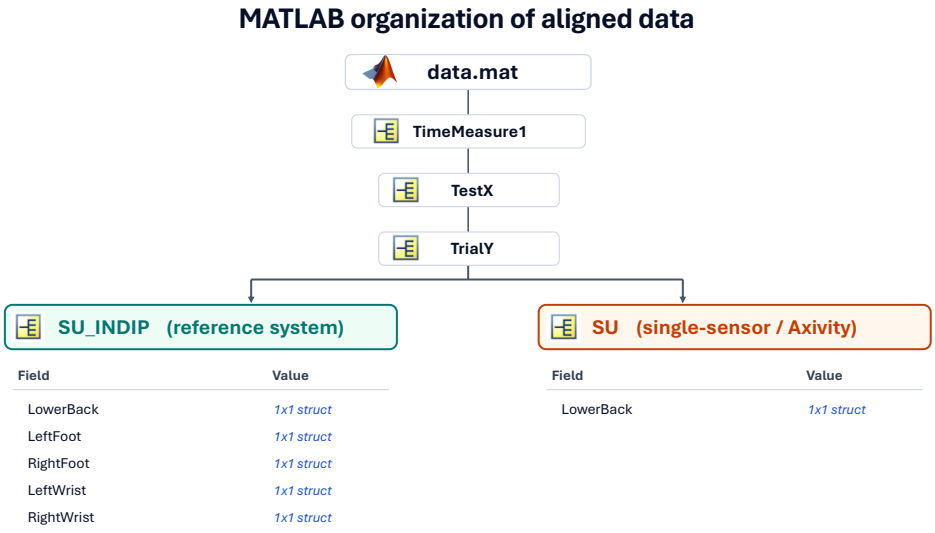


Figure 4.1: Hierarchical organisation of the INDIP and Axivity data within the `data.mat` file. For each test and trial, the multi-sensor INDIP data were stored in the `SU_INDIP` structure, whereas the single-sensor Axivity data were stored in the `SU` structure.

4.1.3 Lower-back sensor reorientation

An additional reorientation procedure was investigated to assess whether deviations of the lower-back sensor from the expected vertical alignment influenced MobGap performance.

The correction was based on the direction of gravity measured during a stationary period. For each walking trial corresponding to Tests 4–7, a stationary window of

at least 3 s was searched within the first and last 10 s of the recording using the gyroscope signal. A window was considered stationary when the 95th percentile of the gyroscope magnitude was below 5 deg/s. If more than one suitable interval was found, the window with the lowest mean gyroscope magnitude was selected.

The mean acceleration vector within the selected interval was used to estimate the direction of gravity. Sensor inclination was quantified as the angle between this direction and the positive X-axis of the expected MobGap sensor frame. When no suitable stationary period could be identified within a walking trial, the gravity direction estimated from Test 2 Trial 1 was used as a fallback.

For each participant, mean sensor inclination was calculated across the available walking trials.

A rotation matrix was then calculated to align the estimated gravity direction with the positive X-axis, corresponding to the vertical axis used by MobGap. The same rotation was applied to both acceleration and angular-velocity signals.

MobGap processing was first performed using the original Axivity signals. The reoriented signals were then processed separately using the same pipeline configuration. This allowed the effect of the additional orientation correction on stride detection and gait-parameter estimation to be evaluated without altering the primary analysis.

4.2 Processing

Following data preparation, INDIP and Axivity recordings were processed independently. INDIP outputs were used as the reference, whereas the Axivity recordings were processed using the single-sensor MobGap pipeline.

The INDIP recordings were processed using the validated in-house pipeline developed for the multi-sensor reference system [19]. The pipeline combines information from the different INDIP sensors to identify continuous walking periods, foot–ground contacts, strides, and turning intervals, and to estimate the corresponding gait parameters. The outputs retained for the present analysis were stride start and end times, stride duration, stride length, and walking speed. Standard INDIP processing scripts were applied without modification.

The aligned lower-back Axivity acceleration and angular-velocity signals were processed in Python using version 1.2.0 of the *mobgap* library [34]. Only the walking tests were included: Timed Up and Go, Straight Walk, 6-Minute Walk Test, and Unstructured Walk. Acceleration was converted from gravitational units to m/s^2, while angular velocity was expressed in deg/s.

Participant height and lower-back sensor height were provided as participant-specific metadata, and the measurement condition was set as laboratory-based. Processing was performed using the `MobilisedPipelineImpaired` pipeline, which

implements the Mobilise-D framework for cohorts with impaired mobility [8].

Since no ataxia-specific configuration was available, the multiple-sclerosis configuration was selected as an available neurological impaired-gait setting within the pipeline. This choice was made only to define the processing configuration and does not imply equivalence between the gait characteristics of the two populations.

The default components of the `MobilisedPipelineImpaired` pipeline were retained except for the laterality-classification algorithm. The default classifier was replaced with `LrcMansour` [35], which assigns a left or right label to each detected initial contact using mediolateral acceleration measured at the lower back. Laterality information was required to associate initial contacts with the corresponding foot and to define complete strides.

This modification was introduced following preliminary inspection of laterality assignments in the present dataset. No formal comparison between `LrcMansour` and the default classifier was performed. Its use should therefore be considered a methodological choice rather than evidence of superior performance in people with ataxia.

For each trial, MobGap returned detected gait sequences, initial contacts, walking bouts, and stride-level parameters. Stride start and end times, stride duration, stride length, and walking speed were retained for comparison with INDIP.

4.2.1 Turn detection

Turning periods were identified using the `TdElGohary` algorithm implemented in MobGap, based on the method proposed by El-Gohary et al. [33]. The algorithm uses the angular velocity measured by the lower-back gyroscope around the vertical axis, since rotation around this axis is the main component of a change in walking direction.

The angular-velocity signal was first low-pass filtered to reduce faster movements not related to the change in direction. Peaks larger than 15 deg/s were considered possible turns. For each peak, the beginning and end of the turn were identified by moving backward and forward in the signal until the angular velocity fell below 5 deg/s.

Turn candidates occurring very close to each other and in the same direction were merged. The total turning angle was then obtained by integrating the angular-velocity signal over the detected interval. Only turns lasting between 0.5 and 10 s and with a rotation of at least 45° were retained.

The final output therefore consisted of the start and end of each detected turning interval, together with its duration, turning angle, and direction. These intervals were later related to the initial contacts delimiting each stride to obtain a stride-level turn label. This label could take the values 0, 0.5, or 1, as described in Section 4.4.2.

4.3 Stride matching

After processing, temporally aligned initial contacts (ICs) and strides were available from both INDIP and MobGap. INDIP was considered the reference system.

Matching was performed in two steps. First, INDIP initial contacts were associated with MobGap initial contacts according to their temporal distance. These associations were then used to determine whether a complete INDIP stride had a corresponding MobGap stride.

4.3.1 Initial contact matching

For each reference IC identified by INDIP, the temporally closest MobGap IC was searched. A temporal acceptance window was defined around each INDIP event as

$$W_i = \left[t_i^{\text{INDIP}} - \tau,\, t_i^{\text{INDIP}} + \tau \right], \tag{4.5}$$

where τ is the maximum accepted temporal difference between the two systems.

The tolerance was selected according to the initial-contact evaluation procedure used in the Mobilise-D validation framework [8]. A 0.5-s acceptance window centred on each reference IC was used in that study. The tolerance applied on either side of the reference event was therefore

$$\tau = 0.25 \text{ s} = 25 \text{ samples}, \qquad f_s = 100 \text{ Hz}. \tag{4.6}$$

For the i-th INDIP IC, the minimum temporal distance from a MobGap IC was

$$d_i = \min_j \left| t_j^{\text{MobGap}} - t_i^{\text{INDIP}} \right|. \tag{4.7}$$

The reference IC was considered matched when

$$d_i \leq \tau. \tag{4.8}$$

If no MobGap IC was found within the acceptance window, the reference event was considered unmatched. The MobGap time associated with each matched INDIP IC was retained for the subsequent stride-matching procedure.

4.3.2 Stride matching

Each INDIP stride was defined by two consecutive initial contacts of the same foot, corresponding to the beginning and end of the stride. A reference stride could only be matched if both delimiting INDIP initial contacts had been successfully associated with MobGap events.

For each eligible INDIP stride, MobGap strides compatible with both boundaries were searched. A candidate MobGap stride was accepted only when its start and end times were within the same tolerance τ of the MobGap initial contacts associated with the reference boundaries.

If more than one candidate was available, the stride with the smallest total temporal difference from the reference boundaries was selected:

$$E_j = \left| t_{\text{start},j}^{\text{MobGap}} - t_{\text{start},i}^{\text{INDIP}} \right| + \left| t_{\text{end},j}^{\text{MobGap}} - t_{\text{end},i}^{\text{INDIP}} \right|. \tag{4.9}$$

Each MobGap stride could be assigned to only one INDIP stride.

A reference stride with a corresponding MobGap stride was classified as a true positive ($\text{TP}_{\text{stride}}$). An INDIP stride without a compatible MobGap stride was classified as a false negative ($\text{FN}_{\text{stride}}$), while a MobGap stride that was not assigned to an INDIP reference stride was classified as a false positive ($\text{FP}_{\text{stride}}$).

The total numbers of strides detected by the two systems were therefore

$$N_{\text{INDIP,stride}} = N_{\text{TP,stride}} + N_{\text{FN,stride}}, \tag{4.10}$$

and

$$N_{\text{MobGap,stride}} = N_{\text{TP,stride}} + N_{\text{FP,stride}}. \tag{4.11}$$

Stride-detection sensitivity was calculated as

$$\text{Sensitivity}_{\text{stride}} = \frac{N_{\text{TP,stride}}}{N_{\text{TP,stride}} + N_{\text{FN,stride}}}, \tag{4.12}$$

while positive predictive value (PPV) was calculated as

$$\text{PPV}_{\text{stride}} = \frac{N_{\text{TP,stride}}}{N_{\text{TP,stride}} + N_{\text{FP,stride}}}. \tag{4.13}$$

Sensitivity represents the proportion of INDIP reference strides that were also detected by MobGap, whereas PPV represents the proportion of MobGap strides that corresponded to an INDIP reference stride.

The percentage of matched reference strides was additionally expressed as

$$P_{\text{matched}} = \frac{N_{\text{TP,stride}}}{N_{\text{INDIP,stride}}} \times 100. \tag{4.14}$$

Only successfully matched stride pairs were retained for the paired evaluation of stride duration, stride length, and walking speed.

4.4 Performance evaluation

MobGap performance was evaluated separately for stride detection and gait-parameter estimation.

Stride-detection performance was described using the number of true-positive, false-negative, and false-positive strides together with sensitivity and PPV, as defined in Section 4.3.

Gait-parameter estimation was evaluated only for successfully matched stride pairs. Each MobGap estimate was therefore compared directly with the corresponding INDIP reference value.

For a generic gait parameter, the signed error of the i-th matched stride was defined as

$$e_i = x_i^{\text{MobGap}} - x_i^{\text{INDIP}}, \tag{4.15}$$

where x_i^{MobGap} is the MobGap estimate and x_i^{INDIP} is the corresponding reference value. Positive values indicate overestimation by MobGap and negative values indicate underestimation.

The mean absolute error (MAE) was calculated as

$$\text{MAE} = \frac{1}{N}\sum_{i=1}^{N}\left|x_i^{\text{MobGap}} - x_i^{\text{INDIP}}\right|, \tag{4.16}$$

where N is the number of matched strides with valid values for the parameter under evaluation.

For each matched stride, the absolute relative error (ARE) was calculated as

$$\text{ARE}_i = 100\frac{\left|x_i^{\text{MobGap}} - x_i^{\text{INDIP}}\right|}{x_i^{\text{INDIP}}}. \tag{4.17}$$

The mean absolute relative error (MARE) was then calculated as

$$\text{MARE} = \frac{1}{N}\sum_{i=1}^{N}\text{ARE}_i. \tag{4.18}$$

Signed errors were summarised using the median and interquartile range and reported as bias. Stride-level ARE values were also reported as median [Q1–Q3].

4.4.1 Stratification by rollator use

To explore whether performance differed during rollator-assisted walking, participants were divided according to rollator use. Participants S3 and S5 formed the rollator group, while S1, S2, and S4 formed the non-rollator group. S2 used a

walking stick and was included in the latter group because the analysis specifically focused on rollator use.

Stride-detection sensitivity and PPV were first calculated for each participant. Group-level values were then obtained by averaging the participant-specific results, so that each participant contributed equally regardless of the number of available strides.

Gait-parameter estimation was evaluated using the matched strides belonging to each group. MARE was calculated separately for stride duration, stride length, and walking speed by pooling the valid matched strides within each group.

The analysis was considered descriptive because rollator use was participant-specific and the same participants were not evaluated both with and without the device. Differences between groups could therefore also reflect individual differences in gait impairment.

4.4.2 Stratification by walking condition: straight and turning strides

To investigate whether estimation performance changed during directional changes, matched strides were classified as straight, turning, or intermediate.

Classification was based on the turning intervals identified by the INDIP reference system. MobGap turn detection was not used to define the reference walking condition in the clinical analysis.

Each reference stride was defined by its two delimiting initial contacts and was classified according to their position relative to the INDIP turning intervals:

$$\text{TurnClass}_i = \begin{cases} 1, & \text{both delimiting ICs fall within a turning interval} \\ 0.5, & \text{only one delimiting IC falls within a turning interval} \\ 0, & \text{neither delimiting IC falls within a turning interval.} \end{cases} \tag{4.19}$$

A value of 1 identified a complete turning stride, a value of 0 identified a complete straight stride, and a value of 0.5 identified an intermediate stride crossing the beginning or end of a turn.

For each matched pair, the class assigned to the INDIP stride was also assigned to the corresponding MobGap stride. Intermediate strides were excluded from the stratified performance analysis, leaving only complete straight and complete turning strides.

Gait-parameter estimation was then evaluated separately for the two conditions. MAE and MARE were calculated for stride duration, stride length, and walking speed, while stride-level ARE values were summarised using the median and interquartile range.

Sensitivity and PPV were not calculated separately for straight and turning strides. Walking condition was defined from the INDIP turning intervals and then transferred to successfully matched MobGap strides, so an independent set of condition-specific MobGap false-positive and false-negative detections was not available.

This analysis was included because turning changes trunk rotation, step geometry, and direction of progression compared with steady-state straight walking, which may affect both gait-event detection and spatial gait-parameter estimation from a lower-back sensor [36, 37].

4.5 Free-living data processing

The 7-day Axivity recordings required a different preprocessing procedure from the clinical recordings. The AX6 recorded continuously throughout the monitoring period and no simultaneous INDIP reference was available. Temporal alignment with INDIP and segmentation into clinical trials were therefore not required.

The continuous Axivity recording was read from the original CWA file and divided into consecutive daily segments. Each recording day was then processed independently using MobGap.

4.5.1 CWA file reading and daily segmentation

The AX6 stores inertial data in the binary CWA format, in which sensor samples and acquisition information are organised in consecutive data blocks. Because the 7-day recordings were large, a dedicated Python script was used to read the files sequentially rather than loading the entire recording into memory.

For each block, the three acceleration and three angular-velocity components were extracted together with their timing information. Acceleration was converted to m/s^2 and angular velocity to deg/s.

The continuous recording was progressively divided into segments of approximately 24 hours. Each segment was treated as one recording day, resulting in a maximum of seven daily datasets for each participant.

4.5.2 Daily MobGap processing

Each daily recording was organised as a six-channel dataset containing the three acceleration and three angular-velocity components. Participant height and lower-back sensor height were provided as participant-specific metadata, while the measurement condition was set as free-living.

The daily datasets were processed independently using the `MobilisedPipelineImpaired` pipeline from MobGap with the same general configuration used for the clinical recordings. The `LrcMansour` algorithm was used for laterality classification, and turn detection was applied within the detected gait sequences.

For each day, MobGap returned gait sequences, initial contacts, turns, strides, walking bouts, and the corresponding stride- and walking-bout-level parameters. The outputs were stored separately for each recording day and subsequently used for the free-living analysis.

4.5.3 Free-living data analysis

Free-living data were available for S1, S2, and S5. The analysis was performed separately for each participant rather than pooling gait-parameter data across subjects. This preserved individual gait characteristics and allowed clinical and free-living measurements to be compared within the same participant.

For each participant, stride duration, stride length, and walking speed were examined across three data sources: INDIP measurements obtained during the clinical walking tests, the corresponding clinical MobGap estimates, and MobGap estimates obtained from the 7-day free-living recordings.

For the free-living recordings, gait-parameter distributions were first obtained using all strides detected by MobGap. A second subset was then created by retaining only strides belonging to walking bouts with 0% detected turning. For stride length and walking speed, a further subset was considered by retaining only strides belonging to 0%-turn walking bouts lasting at least 10 s.

Stride duration was therefore examined for all free-living strides and for the 0%-turn subset. Stride length and walking speed were additionally examined after applying the 10-s minimum walking-bout duration criterion.

A separate analysis was performed to describe how common turning was during free-living walking and how much data would be retained when progressively restricting the accepted amount of turning.

For each participant and recording day, walking bouts were characterised using the `turn_percentage` provided by the MobGap walking-bout output. Cumulative thresholds were considered, beginning with walking bouts containing no detected turning and progressively increasing the maximum accepted turn percentage:

$$0\%,\ 0\text{–}10\%,\ 0\text{–}20\%,\ \ldots,\ 0\text{–}100\%. \tag{4.20}$$

For each threshold, the number of walking bouts with a turn percentage lower than or equal to the corresponding upper limit was calculated. The percentage of retained walking bouts was expressed relative to the total number detected during that recording day:

$$P_{\mathrm{WB},k} = \frac{N_{\mathrm{WB},\,\mathrm{turn}\leq k}}{N_{\mathrm{WB,total}}} \times 100, \tag{4.21}$$

where k is the maximum accepted turn percentage, $N_{\mathrm{WB},\,\mathrm{turn}\leq k}$ is the number of walking bouts meeting that criterion, and $N_{\mathrm{WB,total}}$ is the total number of walking bouts detected during the day.

To summarise this analysis across recording days, the median percentage of retained walking bouts was calculated for each participant at each threshold, together with the corresponding interquartile range. An overall summary was then obtained from the participant-level median values using the median and interquartile range across participants. In this way, each participant contributed equally to the overall result, independently of the number of walking bouts detected.

Chapter 5

Results

5.1 Axivity temporal alignment

Figure 5.1 shows the result of the temporal alignment between the Axivity sensor and the INDIP reference system, performed according to the steps described in Section 4.1.1.

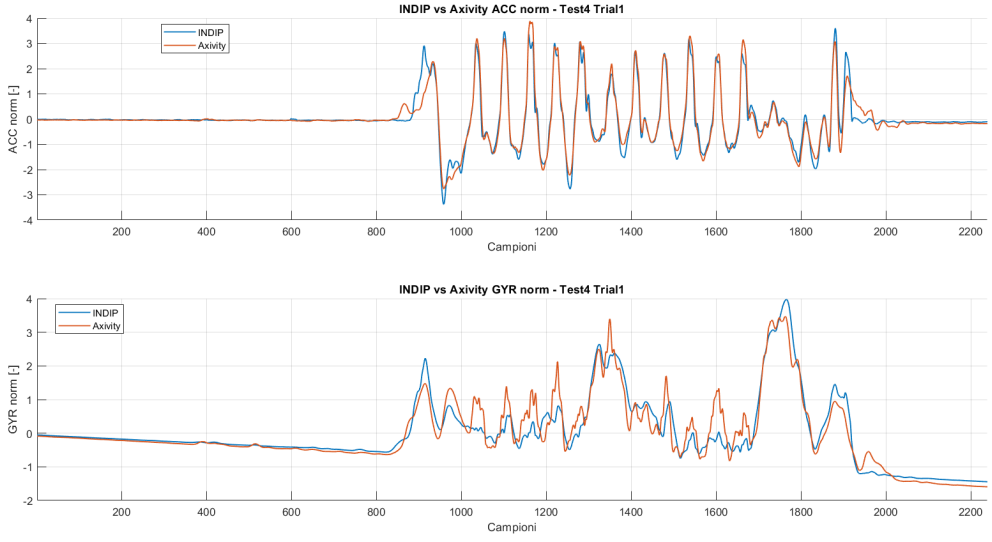


Figure 5.1: Temporal alignment between the Axivity sensor and the INDIP reference system.

5.2 MobGap performance

MobGap performance was first evaluated using the original Axivity sensor orientation. Results are reported separately for each participant, according to rollator use, and overall across all matched strides. Gait-parameter estimation was also examined separately for straight and turning strides.

5.2.1 Participant-specific performance

Stride-detection performance was evaluated separately for each participant. Table 5.1 reports the number of true-positive, false-negative, and false-positive strides together with sensitivity and positive predictive value. Walking aid and mean trunk inclination across the available walking trials are also reported.

Across all participants, INDIP identified 4151 reference strides and MobGap identified 3921 strides. A total of 2876 reference strides were matched with a MobGap stride, corresponding to an overall sensitivity of 69.3% and an overall PPV of 73.3%.

Gait-parameter estimation errors were calculated for the matched stride pairs. Participant-specific results for stride duration, stride length, and walking speed are reported in Table 5.2.

5.2.2 Stratification by rollator use

Participants S3 and S5 were included in the rollator group, while S1, S2, and S4 were included in the non-rollator group.

Mean participant-specific stride-detection sensitivity was 98.9% in the non-rollator group and 54.2% in the rollator group. Mean PPV was 96.6% and 55.3%, respectively.

Gait-parameter estimation also differed between the two groups. Stride-duration MARE was 2.3% in the non-rollator group and 3.0% in the rollator group. Larger differences were observed for the spatial parameters: stride-length MARE was 8.7% in the non-rollator group and 26.8% in the rollator group, while walking-speed MARE was 8.5% and 26.9%, respectively.

5.2.3 Overall gait-parameter estimation performance

Overall gait-parameter estimation performance was evaluated by pooling all valid matched strides across participants. Mean absolute error (MAE), mean absolute relative error (MARE), absolute relative error, and bias were calculated for each gait parameter. ARE and bias are reported as median and interquartile range in Table 5.3.

Table 5.1: Participant-specific stride-detection performance using the original sensor orientation. Mean trunk inclination was calculated across the available walking trials. TP: true positives; FN: false negatives; FP: false positives; PPV: positive predictive value.

Participant	Walking aid	Mean trunk inclination (°)	TP	FN	FP	Sensitivity	PPV
S1–0239	No	10	730	10	10	98.6%	98.6%
S2–807	Stick	22	14	0	1	100.0%	93.3%
S3–192	Rollator	22	239	1160	913	17.1%	20.7%
S4–811	No	14	1019	21	22	98.0%	97.9%
S5–180	Rollator	9	874	84	99	91.2%	89.8%

Table 5.2: Participant-specific gait-parameter estimation errors using the original sensor orientation. Bias and absolute relative error (ARE) are reported as median [Q1–Q3].

Participant	Walking aid	Stride duration		Stride length		Walking speed	
		Bias (ms) median [Q1–Q3]	ARE (%) median [Q1–Q3]	Bias (cm) median [Q1–Q3]	ARE (%) median [Q1–Q3]	Bias (m/s) median [Q1–Q3]	ARE (%) median [Q1–Q3]
S1–0239	No	0.0 [−10.0–10.0]	1.0 [0.9–2.0]	−2.3 [−6.3–2.4]	5.4 [2.6–9.4]	−0.02 [−0.06–0.02]	5.8 [2.7–9.2]
S2–807	Stick	0.0 [−7.5–20.0]	1.9 [0.2–2.0]	−7.6 [−14.0– − 5.5]	6.1 [4.4–10.8]	−0.10 [−0.13– − 0.08]	7.7 [6.8–10.3]
S3–192	Rollator	−10.0 [−30.0–10.0]	1.7 [0.8–2.7]	14.9 [10.1–22.1]	26.1 [16.4–43.0]	0.13 [0.09–0.19]	27.1 [17.3–43.6]
S4–811	No	0.0 [−20.0–20.0]	1.9 [1.0–3.9]	2.5 [−2.1–8.3]	3.8 [1.6–7.7]	0.02 [−0.02–0.07]	3.4 [1.4–6.9]
S5–180	Rollator	0.0 [−30.0–40.0]	2.2 [1.3–4.2]	19.4 [14.9–24.7]	20.5 [15.5–26.9]	0.14 [0.10–0.18]	20.8 [15.6–27.3]

Table 5.3: Overall gait-parameter estimation performance using the original sensor orientation. ARE and bias are reported as median [Q1–Q3].

Parameter	N	MAE	MARE (%)	ARE (%) median [Q1–Q3]	Bias median [Q1–Q3]
Stride duration	2876	31.9 ms	2.6	1.9 [0.9–3.4]	0.0 [−20.0–20.0] ms
Stride length	2868	0.123 m	15.7	9.1 [3.3–20.5]	+0.068 [−0.016–0.184] m
Walking speed	2868	0.095 m/s	15.6	8.5 [3.1–20.9]	+0.055 [−0.015–0.135] m/s

5.2.4 Straight and turning strides

Matched strides were classified according to the INDIP turning intervals. Intermediate strides were excluded from this analysis. Gait-parameter errors were then calculated separately for complete straight and turning strides.

Participant-specific results are reported in Table 5.4.

Overall results for straight and turning strides were calculated by pooling the valid matched strides across participants within each condition and are reported in Table 5.5.

Table 5.5: Overall gait-parameter estimation performance for straight and turning strides using the original sensor orientation. ARE is reported as median [Q1–Q3].

Condition	Parameter	N	MAE	MARE (%)	ARE (%) median [Q1–Q3]
Straight	Stride duration	2375	27.8 ms	2.3	1.7 [0.9–2.9]
	Stride length	2372	0.113 m	13.1	8.1 [3.1–19.4]
	Walking speed	2372	0.087 m/s	13.2	7.8 [2.9–19.7]
Turning	Stride duration	222	54.7 ms	4.2	3.1 [1.6–5.9]
	Stride length	219	0.221 m	40.5	21.8 [7.6–55.0]
	Walking speed	219	0.174 m/s	37.7	19.6 [8.5–53.7]

Table 5.4: Participant-specific gait-parameter estimation errors for straight and turning strides using the original sensor orientation. Only correctly matched strides were included and intermediate strides were excluded. Absolute relative error (ARE) is reported as median [Q1–Q3]. N_{SD} indicates the number of valid stride-duration estimates, while $N_{SL/WS}$ indicates the number of valid stride-length and walking-speed estimates.

Participant	Walking aid	Condition	N_{SD}	$N_{SL/WS}$	SD ARE (%) median [Q1–Q3]	SL ARE (%) median [Q1–Q3]	WS ARE (%) median [Q1–Q3]
S1–0239	No	Straight	609	609	1.0 [0.8–1.9]	5.0 [2.4–7.9]	5.2 [2.5–7.9]
		Turning	61	61	2.2 [0.9–3.7]	21.3 [7.5–51.4]	23.4 [9.4–50.5]
S2–807	Stick	Straight	14	14	1.9 [0.0–2.0]	6.1 [4.3–11.2]	7.7 [6.8–10.4]
		Turning	0	0	–	–	–
S3–192	Rollator	Straight	232	231	1.7 [0.8–2.7]	25.8 [16.3–41.5]	27.1 [17.2–43.2]
		Turning	3	3	1.7 [1.1–1.7]	63.6 [48.1–142.1]	65.8 [43.1–148.8]
S4–811	No	Straight	792	790	1.9 [0.9–3.0]	3.2 [1.5–6.3]	2.9 [1.2–5.3]
		Turning	96	96	3.6 [1.8–6.5]	17.0 [5.6–52.6]	15.2 [7.6–45.0]
S5–180	Rollator	Straight	728	728	2.1 [0.8–3.8]	20.4 [15.9–25.9]	20.8 [15.9–26.2]
		Turning	62	59	3.8 [2.2–7.1]	25.6 [13.5–65.6]	23.5 [12.9–65.6]

5.3 MobGap performance after sensor reorientation

MobGap performance was subsequently re-evaluated after applying the additional lower-back sensor reorientation. As for the analysis performed using the original sensor orientation, results were examined separately for each participant, overall by pooling all matched strides.

5.3.1 Participant-specific performance

Stride-detection performance after lower-back sensor reorientation was evaluated separately for each participant. Walking-aid use and mean trunk inclination across the available walking trials are also reported in Table 5.6.

Gait-parameter estimation errors were then evaluated on correctly matched stride pairs for stride duration, stride length, and walking speed. Participant-specific results are reported in Table 5.7.

5.3.2 Overall gait-parameter estimation performance

Overall gait-parameter estimation performance after sensor reorientation was evaluated by pooling all valid matched strides across participants. Stride-level absolute relative errors were summarised using the median and interquartile range, while the mean absolute relative error (MARE) was calculated across all valid strides for each gait parameter. Results are reported in Table 5.8.

Table 5.8: Overall gait-parameter estimation performance after lower-back sensor reorientation. Absolute relative error (ARE) is reported as median [Q1–Q3]. MARE: mean absolute relative error.

Parameter	**N**	**ARE (%) median [Q1–Q3]**	**MARE (%)**
Stride duration	3402	1.9 [0.9–3.3]	2.5
Stride length	3398	24.3 [16.5–30.7]	27.3
Walking speed	3398	24.8 [16.4–31.4]	28.7

Table 5.6: Participant-specific stride-detection performance after lower-back sensor reorientation. Mean trunk inclination was calculated across the available walking trials. TP: true positives; FN: false negatives; FP: false positives; PPV: positive predictive value.

Participant	Walking aid	Mean trunk inclination (°)	TP	FN	FP	Sensitivity	PPV
S1–0239	No	10	721	19	15	97%	98%
S2–807	Stick	22	14	0	1	100%	93%
S3–192	Rollator	22	1201	198	311	86%	79%
S4–811	No	14	1019	21	21	98%	98%
S5–180	Rollator	9	854	104	110	89%	89%

Table 5.7: Participant-specific gait-parameter estimation errors after lower-back sensor reorientation. Bias and absolute relative error (ARE) are reported as median [Q1–Q3].

Participant	Walking aid	Stride duration		Stride length		Walking speed	
		Bias (ms) median [Q1–Q3]	ARE (%) median [Q1–Q3]	Bias (cm) median [Q1–Q3]	ARE (%) median [Q1–Q3]	Bias (m/s) median [Q1–Q3]	ARE (%) median [Q1–Q3]
S1–0239	No	0.0 [−10.0–10.0]	1.0 [0.9–2.0]	−20.0 [−23.9– − 14.4]	21.7 [17.6–25.2]	−0.19 [−0.23– − 0.13]	22.0 [17.3–25.4]
S2–807	Stick	0.0 [−5.0–30.0]	1.5 [0.0–2.8]	−37.2 [−43.7– − 24.4]	28.8 [19.6–33.6]	−0.37 [−0.42– − 0.25]	29.5 [19.9–34.2]
S3–192	Rollator	0.0 [−20.0–20.0]	1.7 [0.8–3.3]	16.0 [10.7–22.4]	30.0 [19.1–46.6]	0.13 [0.08–0.18]	32.0 [18.1–50.4]
S4–811	No	0.0 [−20.0–20.0]	2.0 [1.0–3.9]	−38.1 [−43.8– − 28.1]	28.3 [23.5–31.1]	−0.37 [−0.43– − 0.27]	28.5 [24.0–31.2]
S5–180	Rollator	0.0 [−30.0–30.0]	2.1 [1.2–3.8]	15.6 [9.6–22.0]	16.6 [9.9–24.5]	0.11 [0.07–0.15]	16.6 [10.0–25.2]

5.4 7-day recordings

The results from the 7-day recordings are reported separately for each participant, without pooling gait-parameter data across subjects.

Free-living recordings were available for participants S1, S2, and S5. No free-living data were available for S3 because of a recording issue, as the device was found to contain no data at the end of the acquisition period. Participant S4 did not complete the prolonged recording because of personal commitments related to an upcoming vacation.

The amount of turning occurring during daily-life walking was first examined for each participant. For each recording day, walking bouts were progressively included according to their turn percentage, starting from bouts with exactly 0% detected turning and subsequently increasing the maximum accepted turn percentage in 10% increments up to 100%. This analysis provides an indication of how the amount of available free-living data increases when progressively less restrictive criteria regarding turning are applied.

The clinical and free-living gait-parameter distributions were then compared. Clinical data included the INDIP reference measurements and the corresponding MobGap estimates. For the free-living recordings, all MobGap strides were first considered. A more restrictive subset included only strides belonging to walking bouts with 0% detected turning. For stride length and walking speed, an additional subset was obtained by retaining, among the 0%-turn walking bouts, only those with a duration of at least 10 s.

5.4.1 Participant S1 – 0239

Figure 5.2 shows the cumulative proportion of free-living walking bouts retained when progressively increasing the maximum accepted turn percentage for participant S1. Each series represents one recording day. The first point corresponds to walking bouts with exactly 0% detected turning, while the subsequent points cumulatively include walking bouts with turn percentages up to 10%, 20%, and progressively up to 100%.

Figures 5.3–5.5 show the distributions of stride duration, stride length, and walking speed for S1. The first two distributions represent the clinical measurements obtained with INDIP and MobGap, while the remaining distributions refer to the 7-day MobGap recording.

For stride duration, all free-living strides are compared with the subset belonging to walking bouts with 0% detected turning. For stride length and walking speed, a further restriction is shown by considering only strides from 0%-turn walking bouts lasting at least 10 s.

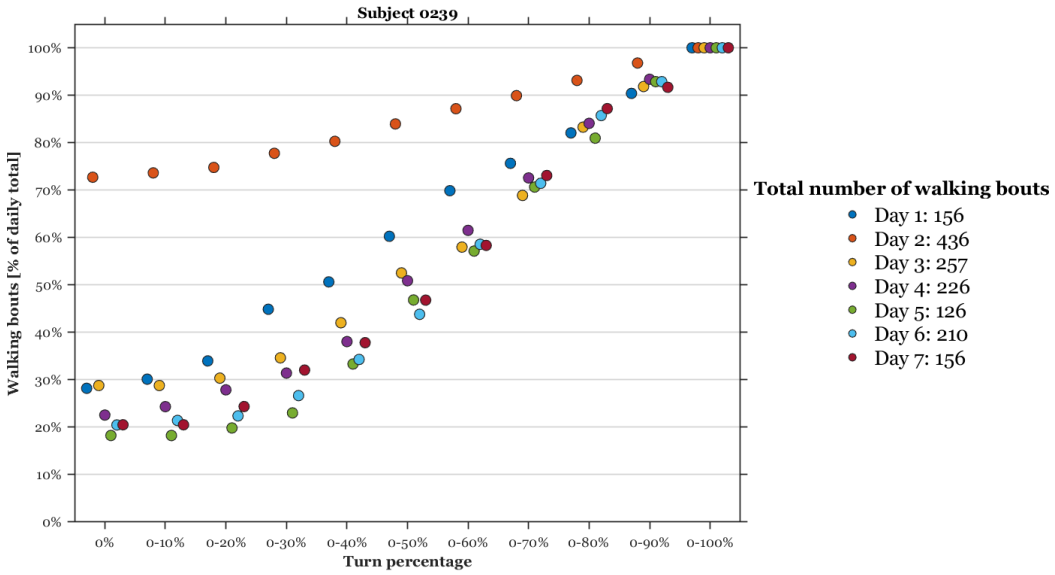


Figure 5.2: Cumulative distribution of walking bouts according to turn percentage for participant S1 (0239). Each series represents one recording day. The first point includes only walking bouts with 0% detected turning, while subsequent thresholds progressively include walking bouts with increasing turn percentages up to 100%. The vertical axis represents the percentage of walking bouts relative to the total number detected on each day.

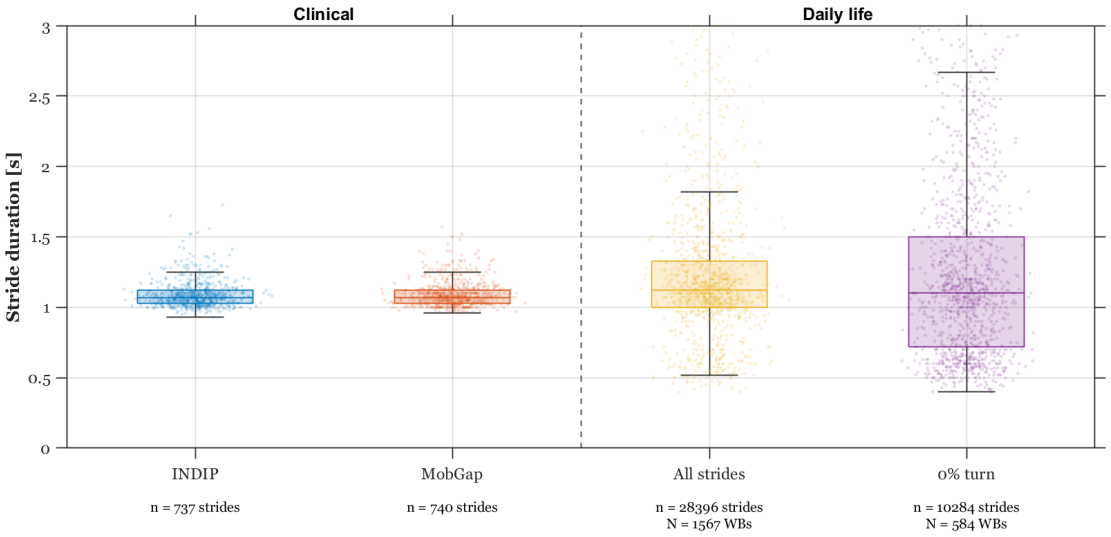


Figure 5.3: Stride duration for participant S1 (0239). Clinical distributions are shown for INDIP and MobGap. Daily-life distributions include all MobGap strides and the subset belonging to walking bouts with 0% detected turning.

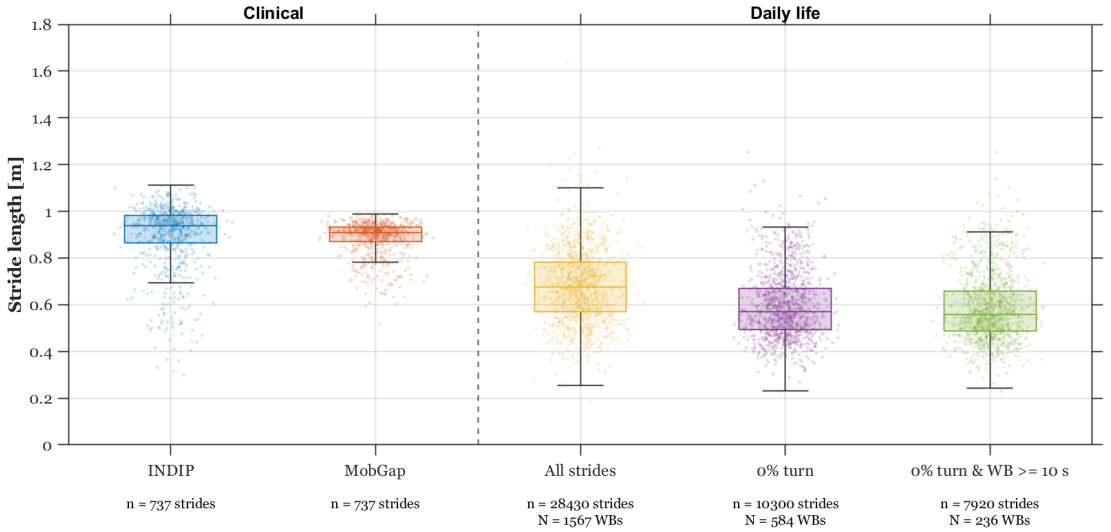


Figure 5.4: Stride length for participant S1 (0239). Clinical distributions are shown for INDIP and MobGap. Daily-life distributions include all MobGap strides, strides from walking bouts with 0% detected turning, and the subset of 0%-turn walking bouts lasting at least 10 s.

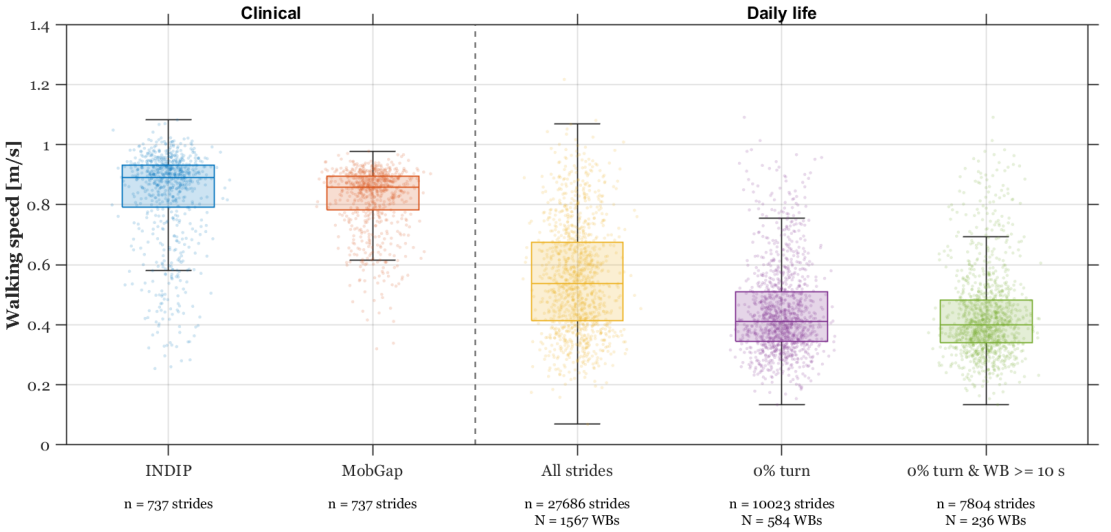


Figure 5.5: Walking speed for participant S1 (0239). Clinical distributions are shown for INDIP and MobGap. Daily-life distributions include all MobGap strides, strides from walking bouts with 0% detected turning, and the subset of 0%-turn walking bouts lasting at least 10 s.

5.4.2 Participant S2 – 807

Figure 5.6 shows the cumulative proportion of free-living walking bouts retained at increasing turn-percentage thresholds for participant S2 across the available recording days.

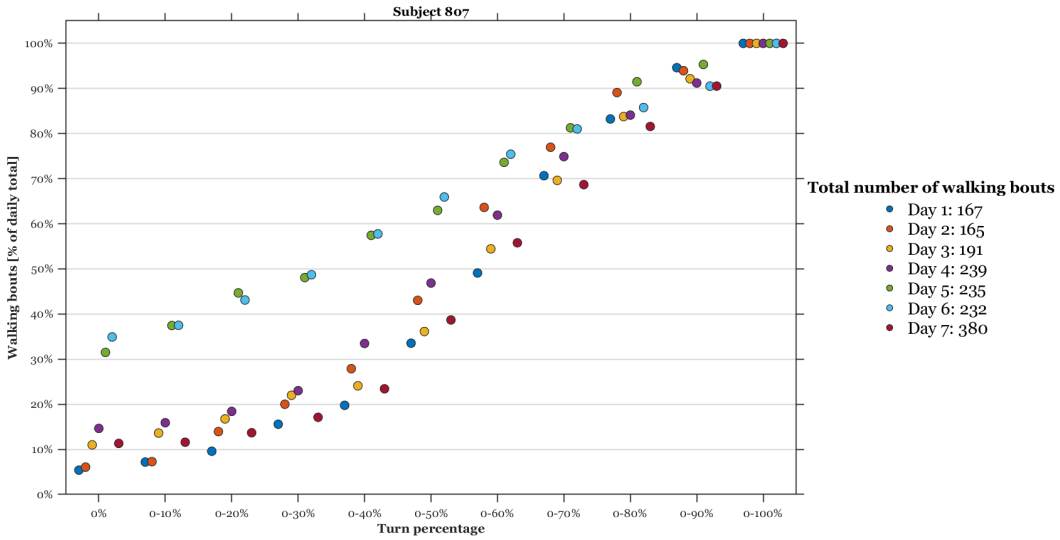


Figure 5.6: Cumulative distribution of walking bouts according to turn percentage for participant S2 (807). Each series represents one recording day. Walking bouts are progressively included from those with 0% detected turning up to a maximum accepted turn percentage of 100%. The vertical axis represents the percentage of walking bouts relative to the total number detected on each day.

Figures 5.7–5.9 show the corresponding clinical and free-living gait-parameter distributions. The available clinical data were obtained from the 10-m Straight Walk, while the free-living distributions were obtained from the 7-day MobGap recording.

As for S1, stride duration is reported both for all free-living strides and for the subset belonging to walking bouts with 0% detected turning. For stride length and walking speed, the additional subset of 0%-turn walking bouts lasting at least 10 s is also shown.

5.4.3 Participant S5 – 180

Figure 5.10 shows the cumulative proportion of free-living walking bouts retained at increasing turn-percentage thresholds for participant S5 across the available recording days.

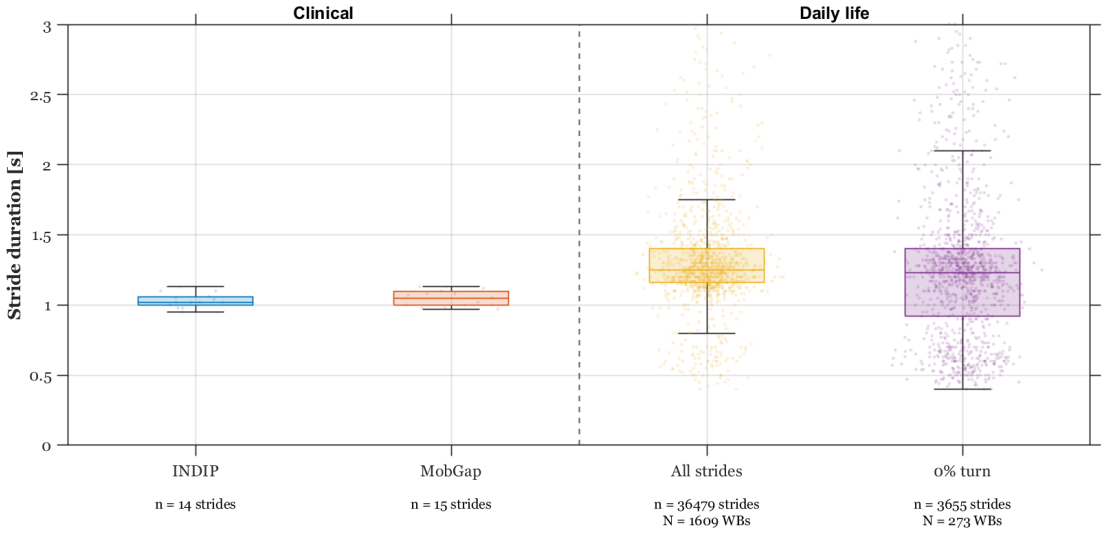


Figure 5.7: Stride duration for participant S2 (807). Clinical distributions are shown for INDIP and MobGap. Daily-life distributions include all MobGap strides and the subset belonging to walking bouts with 0% detected turning.

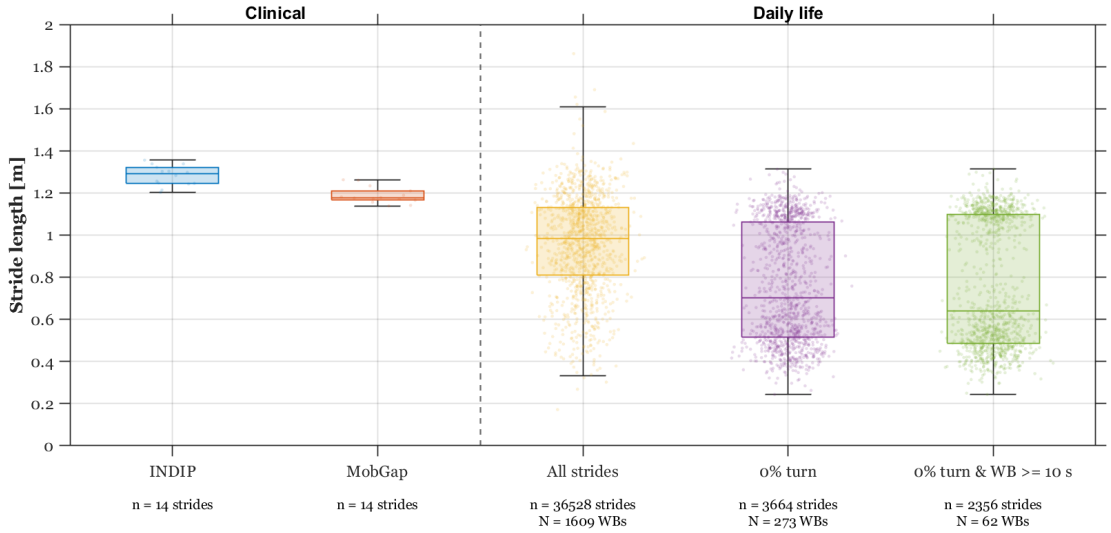


Figure 5.8: Stride length for participant S2 (807). Clinical distributions are shown for INDIP and MobGap. Daily-life distributions include all MobGap strides, strides from walking bouts with 0% detected turning, and the subset of 0%-turn walking bouts lasting at least 10 s.

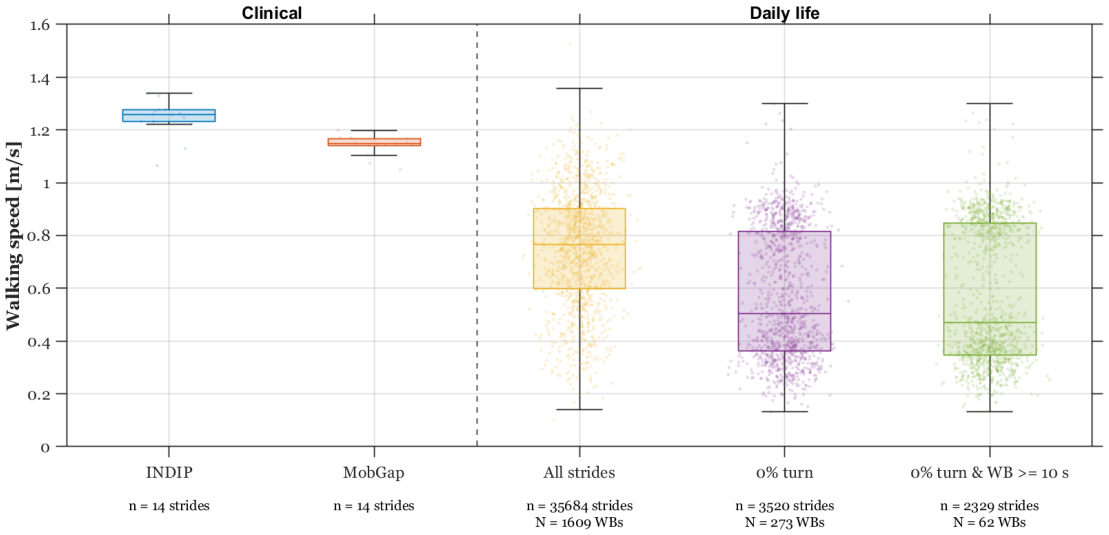


Figure 5.9: Walking speed for participant S2 (807). Clinical distributions are shown for INDIP and MobGap. Daily-life distributions include all MobGap strides, strides from walking bouts with 0% detected turning, and the subset of 0%-turn walking bouts lasting at least 10 s.

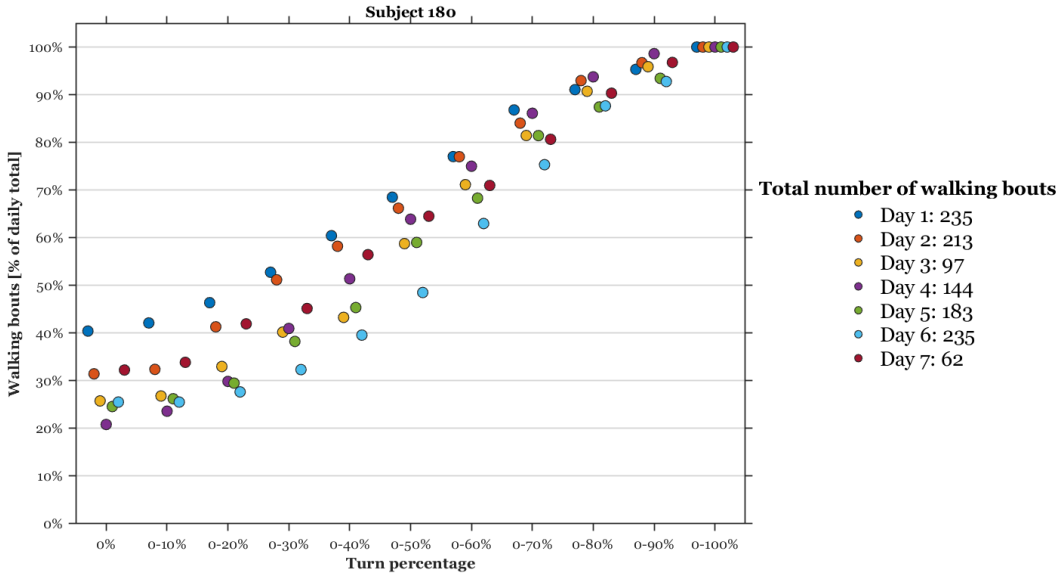


Figure 5.10: Cumulative distribution of walking bouts according to turn percentage for participant S5 (180). Each series represents one recording day. Walking bouts are progressively included from those with 0% detected turning up to a maximum accepted turn percentage of 100%. The vertical axis represents the percentage of walking bouts relative to the total number detected on each day.

Figures 5.11–5.13 show the clinical and free-living gait-parameter distributions obtained for participant S5.

Stride duration is reported for all free-living strides and for the subset belonging to walking bouts with 0% detected turning. For stride length and walking speed, the analysis additionally shows the subset obtained by retaining only 0%-turn walking bouts lasting at least 10 s.

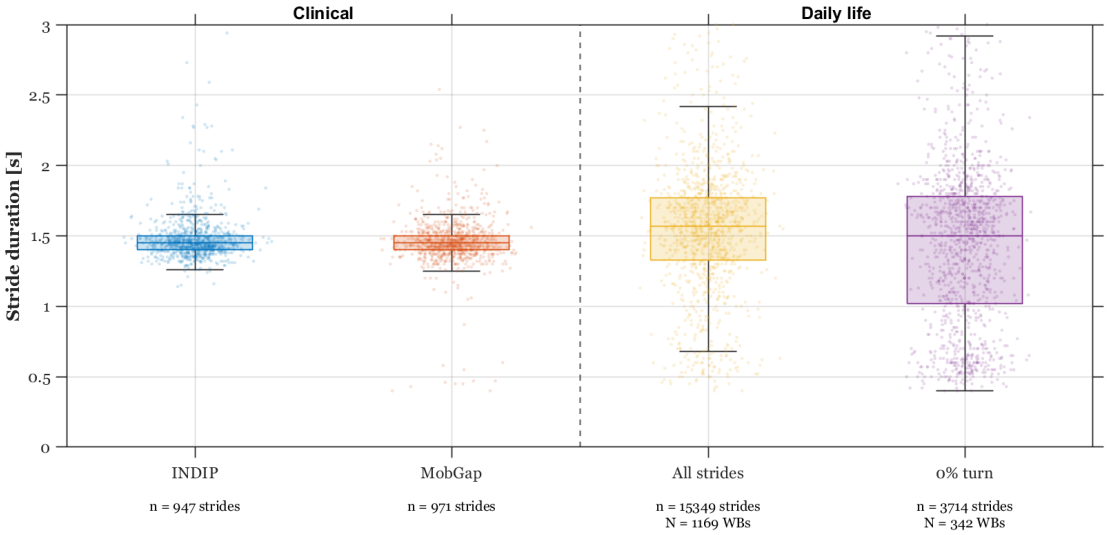


Figure 5.11: Stride duration for participant S5 (180). Clinical distributions are shown for INDIP and MobGap. Daily-life distributions include all MobGap strides and the subset belonging to walking bouts with 0% detected turning.

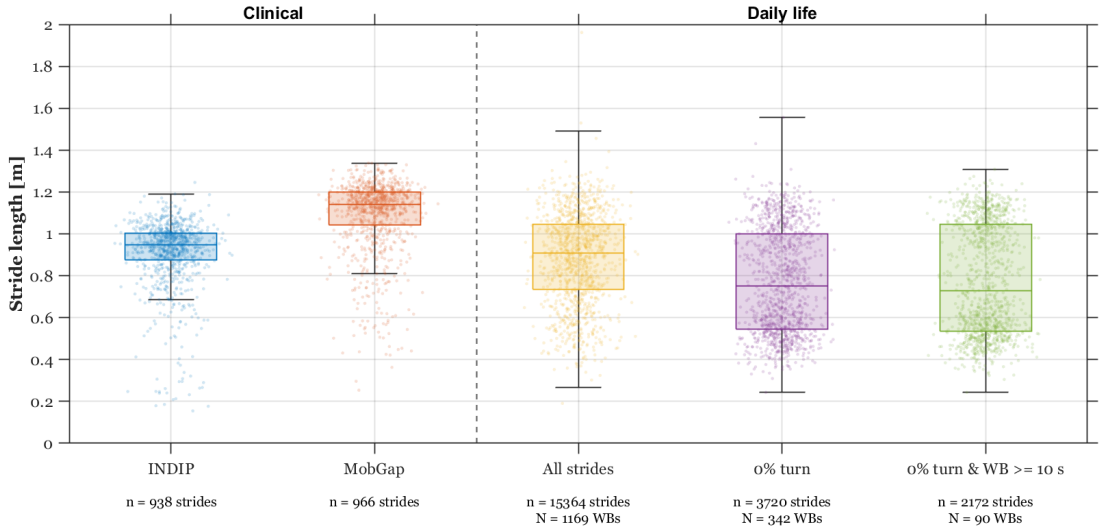


Figure 5.12: Stride length for participant S5 (180). Clinical distributions are shown for INDIP and MobGap. Daily-life distributions include all MobGap strides, strides from walking bouts with 0% detected turning, and the subset of 0%-turn walking bouts lasting at least 10 s.

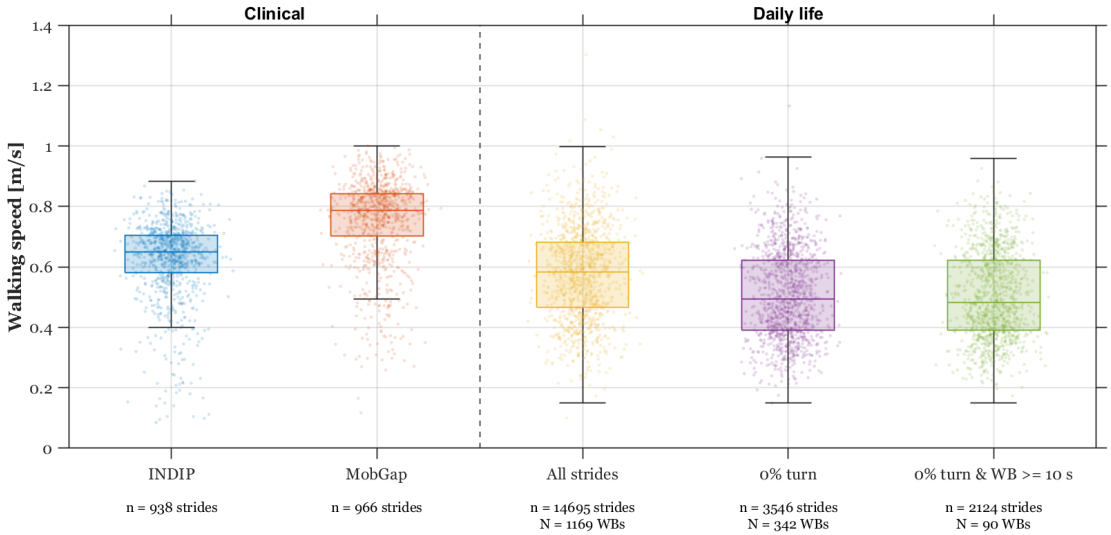


Figure 5.13: Walking speed for participant S5 (180). Clinical distributions are shown for INDIP and MobGap. Daily-life distributions include all MobGap strides, strides from walking bouts with 0% detected turning, and the subset of 0%-turn walking bouts lasting at least 10 s.

5.4.4 Overall turn distribution

Figure 5.14 provides an overall summary of the relationship between the maximum accepted turn percentage and the proportion of free-living walking bouts retained in the analysis.

For each participant, the median proportion of retained walking bouts across the available recording days was calculated at each turn-percentage threshold, together with the corresponding interquartile range. The upper panel shows these participant-specific results. The lower panel provides an overall summary across participants, obtained from the participant-level median values so that each participant contributes equally to the overall distribution.

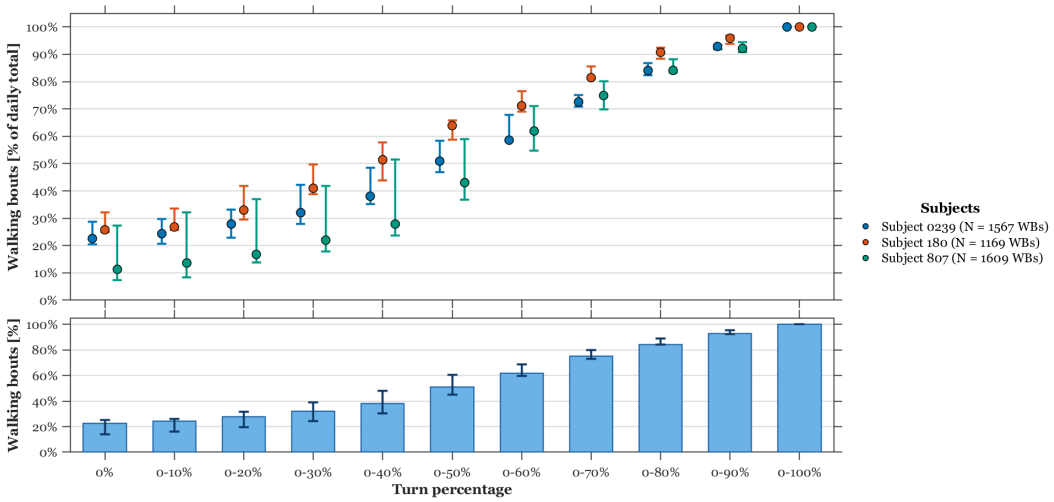


Figure 5.14: Overall cumulative distribution of free-living walking bouts according to the maximum accepted turn percentage. In the upper panel, points represent the median percentage of retained walking bouts across recording days for each participant, with error bars indicating the interquartile range. The lower panel reports the median across participant-level values, with the corresponding interquartile range. Each participant therefore contributes equally to the overall summary.

Chapter 6

Discussion

6.1 Overall MobGap performance in people with ataxia

The main aim of this study was to evaluate MobGap performance in people with ataxia using a single lower-back inertial sensor. The analysis first considered stride detection and then the accuracy of the estimated gait parameters.

Using the original sensor orientation, INDIP identified 4151 reference strides, while MobGap identified 3921 strides. A total of 2876 reference strides were successfully matched, resulting in an overall sensitivity of 69.3% and a PPV of 73.3%. These values were strongly influenced by participant S3. For the other participants, sensitivity ranged from 91.2% to 100% and PPV from 89.8% to 98.6%. In contrast, S3 showed a sensitivity of 17.1% and a PPV of 20.7%. The lower overall detection performance was therefore mainly related to this participant.

Gait-parameter errors were calculated only for successfully matched strides. Therefore, these results describe the accuracy of MobGap when a stride was detected by both systems. Missed reference strides were not included in the estimation-error analysis.

For the matched strides, stride duration showed the lowest error, with a MAE of 31.9 ms and a MARE of 2.6%. Stride-length MAE was 0.123 m, with a MARE of 15.7%, while walking-speed MAE was 0.095 m/s, with a MARE of 15.6%.

In addition to MAE and MARE, stride-level errors were reported using the median and interquartile range. No assumption of a normal error distribution was made in this study, and no inferential statistical analysis was performed. The median was therefore used as a robust descriptive measure, since it is less affected by extreme values and asymmetric error distributions than the mean. MAE and MARE were retained mainly to allow a direct comparison with previous Mobilise-D studies.

The results were in line with those previously reported within Mobilise-D, despite the fact that people with ataxia were not included in the original validation cohorts. The clearest comparison can be made for walking speed. Kirk et al. reported laboratory MAE values between 0.06 and 0.12 m/s across the different clinical cohorts [38]. When all true-positive walking bouts were pooled, walking-speed MAE was 0.10 m/s and MARE was 14.96%. In the present study, the corresponding values were 0.095 m/s and 15.6%. The errors were therefore almost identical in magnitude.

The comparison is not completely equivalent because Kirk et al. evaluated walking speed at walking-bout level, while the present study used individual matched strides. However, both analyses used INDIP as the reference and a single lower-back sensor within the Mobilise-D framework [8]. The comparison therefore gives a useful indication of the magnitude of the observed error.

Stride-length results showed the same trend. In the Mobilise-D real-world validation, stride-length absolute errors were approximately 0.15–0.21 m, with relative errors of about 25–34% depending on the cohort [8]. In this study, stride-length MAE was 0.123 m and MARE was 15.7%. The errors were therefore not higher than those previously reported. A direct numerical comparison should still be interpreted carefully because the Mobilise-D values were obtained from real-world recordings and at a different analysis level.

A clear difference was observed between temporal and spatial parameters. Stride duration had a MARE of only 2.6%, compared with 15.7% for stride length and 15.6% for walking speed. A similar pattern was reported in Mobilise-D. Kirk et al. found a laboratory MARE of approximately 4% for cadence and about 14% for stride length, with walking-speed error mainly related to the spatial component [38]. Although cadence and stride duration are not the same parameter, both results indicate that temporal gait information was estimated more accurately than spatial information.

The results on matched strides therefore showed errors of the same order as those reported in previous Mobilise-D populations. However, estimation accuracy and stride detection need to be considered together. MobGap estimated gait parameters accurately when strides were successfully identified, but detection performance was not equally good in all participants. The following analyses were therefore used to investigate some of the conditions that may have affected this performance.

6.2 Influence of rollator use and walking condition on MobGap performance

Two participants, S3 and S5, walked with a rollator. The non-rollator group included S1, S2 and S4. S2 used a walking stick but was included in this group because the analysis specifically focused on rollator use. The two groups were therefore fairly balanced in terms of number of participants. However, the amount of available data was not equally distributed. Only 14 matched strides were available for S2. S3 also contributed fewer matched strides in the original analysis because of its low stride-detection performance. For this reason, the comparison between the two groups should be considered descriptive.

Performance was lower in the rollator group. Mean participant-specific sensitivity decreased from 98.9% in the non-rollator group to 54.2% in the rollator group, while PPV decreased from 96.6% to 55.3%. The difference was small for stride duration, with a MARE of 2.3% without a rollator and 3.0% with a rollator. A much larger difference was found for stride length and walking speed. Stride-length MARE increased from 8.7% to 26.8%, while walking-speed MARE increased from 8.5% to 26.9%.

The participant-specific results showed the same trend. S3 and S5 had the largest errors for stride length and walking speed. For stride length, median ARE was 26.1% in S3 and 20.5% in S5, compared with values between 3.8% and 6.1% in the other participants. Walking-speed errors showed a similar pattern. The error distributions were also wider in the two rollator users, especially in S3. Stride-length ARE in S3 was 26.1% [16.4–43.0], while walking-speed ARE was 27.1% [17.3–43.6]. This suggests that the error was not only larger, but also less consistent across strides.

Previous studies have also reported difficulties when walking aids are used. Soltani et al. found larger errors for participants using walking aids when gait parameters were estimated from a lower-back sensor [39]. In this group, the reported RMSE reached 0.18 m for step length and 0.27 m/s for walking speed. These values cannot be directly compared with the present results because a different error metric was used, but the same general trend was observed.

A similar point was reported within Mobilise-D. Walking-aid use was not analysed separately, but lower performance was found in the cohort with more severe gait impairment [8]. Short walking bouts and walking speeds below 0.5 m/s were also associated with lower algorithm performance. Kirk et al. similarly reported lower walking-speed errors in cohorts with less severe gait impairment [38]. This suggests that more impaired and less regular gait may be more difficult to analyse using a single lower-back sensor.

The rollator itself may also affect the signal measured at the lower back. Alkjær

et al. showed that rollator walking changes lower-limb biomechanics and posture [28]. These changes can modify trunk motion and may affect the estimation of spatial gait parameters from a lower-back sensor. However, in this study the effect of the rollator cannot be separated from the characteristics of the individual participants. S3 and S5 may also have had more severe gait impairment than the other participants.

Walking condition also influenced MobGap performance. Stride-duration MARE increased from 2.3% during straight walking to 4.2% during turning. The increase was much larger for stride length, from 13.1% to 40.5%, and for walking speed, from 13.2% to 37.7%.

The median errors showed the same difference. For stride length, median ARE increased from 8.1% [3.1–19.4] during straight walking to 21.8% [7.6–55.0] during turning. For walking speed, it increased from 7.8% [2.9–19.7] to 19.6% [8.5–53.7]. The interquartile ranges were also much wider during turning, showing that spatial estimation became less consistent when the walking direction changed. Stride duration was less affected, with median ARE increasing from 1.7% [0.9–2.9] to 3.1% [1.6–5.9].

Other studies using lower-back inertial sensors have reported similar results. Pham et al. found lower step-detection performance during turning than during non-turning walking [36]. Kvist et al. also showed that spatial gait estimates were more affected by continuous turning, while temporal parameters remained more stable [37].

In this dataset, stride length and walking speed were more affected by walking condition than stride duration. Both rollator use and turning were associated with larger and more variable errors. This is particularly relevant for the free-living recordings, where these conditions occur naturally and are part of the participant's usual walking behaviour.

6.3 Effect of lower-back sensor reorientation

The participant-specific results suggested that sensor orientation may have contributed to the poor stride-detection performance observed in S3. As shown in Table 5.1, S3 had a mean trunk inclination of 22° and by far the lowest detection performance. Sensitivity was 17.1% and PPV was 20.7%. This was the main reason for testing an additional reorientation of the lower-back sensor signals.

An inclination of 22° was also obtained for S2, but this value should be interpreted with caution. Only one walking trial was available for this participant and no sufficiently long stationary period was found within the recording. The inclination was therefore estimated from the standing calibration trial. It was not possible to verify whether the same orientation was maintained during walking.

After reorientation, stride-detection performance remained almost unchanged in S1, S2, S4 and S5. These participants already showed good results with the original signals. The main change was observed in S3. Sensitivity increased from 17.1% to 86% and PPV from 20.7% to 79%. The number of matched strides increased from 239 to 1201, as reported in Table 5.6. This suggests that sensor orientation was an important factor in the poor stride detection initially observed for this participant.

The effect on gait-parameter estimation was different. Stride-duration MARE remained almost unchanged, decreasing from 2.6% to 2.5%. In contrast, stride-length MARE increased from 15.7% to 27.3%, while walking-speed MARE increased from 15.6% to 28.7%.

The larger number of matched strides after reorientation partly affected these overall values. The total increased from 2876 to 3402, mainly because many more strides from S3 were detected. However, this does not fully explain the increase in spatial errors. Stride-length median ARE also increased in participants who already showed good performance with the original signals. It increased from 5.4% to 21.7% in S1, from 6.1% to 28.8% in S2, and from 3.8% to 28.3% in S4.

The additional reorientation used in this study is not part of the standard MobGap impaired pipeline. In the standard configuration, the stride-length algorithm is applied without an additional orientation-estimation step. Mobilise-D also did not systematically correct small deviations of the sensor from the expected anatomical orientation during data standardisation [40].

This may help explain why the correction did not improve spatial estimates. MobGap estimates stride length from the vertical component of lower-back acceleration. This signal is integrated to estimate vertical displacement, which is then used in the inverted-pendulum model for step-length estimation. Reorienting the sensor changes how the measured acceleration is projected onto the vertical axis. It does not increase the total acceleration, but it can change the amplitude of the component used by the algorithm.

With the original orientation, the overall bias was already positive for stride length and walking speed, indicating a tendency towards overestimation. Changing the vertical component may therefore have further modified the estimated vertical displacement and, consequently, the spatial estimates. However, the effect was not the same in all participants, and after reorientation both overestimation and underestimation were observed. The increase in error should therefore not be interpreted simply as an amplification of the original bias.

The results suggest that correcting sensor inclination from gravity alone is not necessarily beneficial. In S3 it substantially improved stride detection, but the same correction worsened stride-length and walking-speed estimation in several participants. For this dataset, the original MobGap configuration was therefore more reliable for spatial gait-parameter estimation.

6.4 Free-living gait assessment

Free-living recordings were available for S1, S2 and S5. These data provide an exploratory view of how the same participants walked outside the clinical setting. No INDIP reference was available during the 7-day recordings, so the results in this section are based only on MobGap estimates.

The participant-specific distributions in Figures 5.3–5.13 show a clear difference between clinical and daily-life walking. In all three participants, stride length and walking speed were generally lower during free-living walking. This difference was particularly evident in S1 and S2. In S1, the clinical stride-length distribution was centred around 0.9 m, while the free-living distributions were shifted towards shorter strides. Walking speed showed the same behaviour, decreasing from approximately 0.8–0.9 m/s during the clinical tests to lower values in daily life. For S2, the difference was even larger, although only 14 matched clinical strides were available and this comparison should therefore be interpreted with caution. S5 showed the same general tendency, especially for walking speed.

Stride duration showed a less marked shift between the two settings. The main difference was the larger spread of the free-living distributions. This was also visible for stride length and walking speed. The clinical distributions were relatively compact, while the daily-life boxplots covered a much wider range of values. This is expected to some extent, since daily-life walking includes many different situations that are not present during a prescribed clinical test.

In the boxplots, the central line represents the median, while the box extends from the first to the third quartile. The whiskers extend to the most extreme observations within 1.5 times the interquartile range below Q1 and above Q3. Values outside these limits are shown separately. The wider boxes and whiskers observed in the free-living data therefore indicate a greater dispersion of the estimated gait parameters.

The lower stride length and walking speed observed in daily life are also consistent with previous work on ataxia. Pau et al. reported a mean stride length of 0.86 m and a gait speed of 0.73 m/s in people with SCA38 [41]. Casey et al. reported daily-life values of approximately 1.00 m for stride length and 0.93 m/s for walking speed in people with Friedreich ataxia [42]. These values cannot be directly compared with the present data because the populations and measurement methods were different, but they confirm that short strides and reduced walking speed are common features of ataxic gait.

The difference between clinical and daily-life walking is also in agreement with previous wearable studies. Ilg et al. showed that real-life gait contains characteristics that are not fully represented during controlled walking [7]. More recently, Shah et al. found differences in 13 of the 17 gait measures analysed when comparing prescribed clinical walking with one week of daily-life monitoring in

people with spinocerebellar ataxia [27]. The clinical test and the 7-day recording should therefore not be expected to provide the same gait distributions.

Turning was then considered because the clinical analysis showed much larger spatial errors during turns. Figure 5.14 shows how much free-living data remain when the maximum accepted turn percentage is progressively increased. In the upper panel, each point represents the median percentage of retained walking bouts across recording days for one participant, while the error bars represent the corresponding interquartile range. The lower panel gives the same information across participants, again using the median and interquartile range.

The figure shows that walking bouts without any detected turn represent only a limited part of daily-life walking. At the 0% threshold, roughly one quarter of the walking bouts were retained overall. S2 had the lowest proportion, close to 10%, whereas the values for S1 and S5 were around 20–30%. When walking bouts containing up to 50% turning were accepted, about half of the data were retained. A threshold of approximately 70% was needed to retain around three quarters of the walking bouts.

This result is important because it shows how common turning is during free-living walking. Completely excluding turns would remove most of the available walking bouts, particularly for S2. The same effect can be seen when looking at the number of strides retained in the participant-specific plots. For stride length, selecting only 0%-turn walking bouts retained approximately 36% of the original strides for S1, 10% for S2 and 24% for S5. When a minimum walking-bout duration of 10 s was added, these proportions decreased further to approximately 28%, 6% and 14%.

Interestingly, applying these restrictions did not make the free-living distributions more similar to the clinical ones. In several cases, the 0%-turn distributions were shifted towards even shorter stride lengths and lower walking speeds. This is clearly visible for S1 and S2 and is also present, although less marked, in S5. Removing turns therefore does not simply produce a cleaner version of the complete daily-life distribution. It selects a different subset of walking.

The 10-s restriction had a similar effect. It reduced the amount of available data considerably, but it did not bring stride length or walking speed back towards the clinical values. Longer straight walking bouts therefore represent only one part of daily-life mobility and should not be considered equivalent to the walking performed during the clinical tests.

These results should still be interpreted carefully. No reference system was available during the 7-day recordings, so it is not possible to separate true changes in gait from changes in MobGap performance. This is relevant because the clinical analysis showed larger spatial errors during turning and in the participants using a rollator. The wider free-living distributions may therefore reflect both the greater variability of daily-life walking and variability in the algorithm estimates.

For this reason, simply pooling all free-living strides may hide differences related to walking context. At the same time, applying very strict selection criteria removes a large part of the participant's habitual walking. The free-living analysis therefore shows the importance of considering the context in which each walking bout occurs when interpreting gait parameters obtained over prolonged recordings.

Chapter 7

Conclusion

7.1 General results

This thesis evaluated the performance of the MobGap pipeline in people with ataxia using a single inertial sensor placed on the lower back.

When strides were correctly detected and matched with the INDIP reference, the errors for stride duration, stride length and walking speed were comparable with those previously reported within Mobilise-D in other clinical populations. Stride duration was the most accurately estimated parameter, while larger errors were found for stride length and walking speed.

Performance was not the same in all participants and walking conditions. Lower stride-detection performance and larger spatial errors were observed in the participants using a rollator. Turning also increased the error, especially for stride length and walking speed. These results show that the walking condition has an important effect on the estimates obtained from a single lower-back sensor.

Sensor orientation was another relevant aspect. In S3, reorientation strongly improved stride detection, increasing sensitivity from 17.1% to 86% and PPV from 20.7% to 79%. However, applying the same correction to all participants increased the error of the spatial parameters. The reorientation procedure should therefore not be applied systematically without first identifying when it is actually needed.

The 7-day recordings showed clear differences between clinical and daily-life walking. Free-living gait was generally characterised by shorter strides and lower walking speeds, with wider distributions than those observed during the clinical tests. The analysis also showed that removing walking bouts containing turns can strongly reduce the amount of available data. In some participants, only a small proportion of daily-life walking remained after applying strict selection criteria.

The results of this preliminary study support the use of MobGap in people with ataxia, but they also show that the output should be interpreted together with the

walking condition and the quality of the sensor placement.

7.2 Further improvements

The main limitation of this study is the small number of participants. Only five people with ataxia were included, and the amount of available data was not balanced across subjects. In particular, only 14 matched strides were available for S2. The cohort also included different levels of mobility impairment, with two participants using a rollator and one using a walking stick.

A larger cohort would allow the present results to be confirmed across different levels of gait impairment. It would also make it possible to investigate more clearly the effect of walking aids and turning without these factors being strongly linked to individual participants.

An important future step would be to define how much turning can be accepted in a walking bout before the estimation error becomes too large. In this study, spatial errors increased during turning, but excluding all walking bouts containing turns removed a large part of the free-living data. A larger dataset could therefore be used to identify a turn-percentage threshold that provides an acceptable compromise between estimation error and the amount of data retained.

Sensor reorientation should also be investigated further. The results from S3 showed that correcting the sensor orientation can substantially improve stride detection when the sensor is strongly inclined. However, applying the same correction to all participants worsened stride-length and walking-speed estimation. Future work could therefore investigate whether reorientation should only be applied above a certain inclination threshold.

An inclination around 20° could be explored as a possible starting point, since the largest improvement after reorientation was observed in a participant with an inclination of about 22°. The present dataset is not sufficient to define such a threshold, especially because a similar inclination was estimated for S2 and this value could not be reliably verified during walking. More participants with different sensor inclinations would therefore be needed to determine whether a threshold can be identified and whether selective reorientation improves performance.

These two aspects, turn percentage and sensor inclination, could help define more practical rules for analysing free-living data with MobGap in people with ataxia.

Bibliography

[1] Sheng-Han Kuo. «Ataxia». In: *Continuum* 25.4 (2019), pp. 1036–1054. DOI: 10.1212/CON.0000000000000753 (cit. on pp. 1, 2).

[2] Sara Radmard, Theresa A. Zesiewicz, and Sheng-Han Kuo. «Evaluation of Cerebellar Ataxic Patients». In: *Neurologic Clinics* 41.1 (2023), pp. 21–44. DOI: 10.1016/j.ncl.2022.05.002 (cit. on pp. 1, 2).

[3] Thomas Klockgether, Caterina Mariotti, and Henry L. Paulson. «Spinocerebellar Ataxia». In: *Nature Reviews Disease Primers* 5.1 (2019), p. 24. DOI: 10.1038/s41572-019-0074-3 (cit. on p. 2).

[4] Pierre Cabaraux, Sunil K. Agrawal, Huaying Cai, et al. «Consensus Paper: Ataxic Gait». In: *The Cerebellum* 22 (2023), pp. 394–430. DOI: 10.1007/s12311-022-01373-9 (cit. on pp. 2, 3, 9).

[5] Winfried Ilg et al. «Quantitative Gait and Balance Outcomes for Ataxia Trials: Consensus Recommendations by the Ataxia Global Initiative Working Group on Digital-Motor Biomarkers». In: *The Cerebellum* 23 (2024), pp. 1566–1592. DOI: 10.1007/s12311-023-01625-2 (cit. on pp. 2, 3, 9, 16–18).

[6] Tanja Schmitz-Hübsch et al. «Scale for the assessment and rating of ataxia: Development of a new clinical scale». In: *Neurology* 66.11 (2006), pp. 1717–1720. DOI: 10.1212/01.wnl.0000219042.60538.92 (cit. on p. 2).

[7] Winfried Ilg, Jens Seemann, Martin A. Giese, Andreas Traschütz, Ludger Schöls, Dagmar Timmann, and Matthis Synofzik. «Real-life gait assessment in degenerative cerebellar ataxia: Toward ecologically valid biomarkers». In: *Neurology* 95.9 (2020), e1199–e1210. DOI: 10.1212/WNL.0000000000010176 (cit. on pp. 3, 9, 17–19, 66).

[8] M. Encarna Micó-Amigo, Tecla Bonci, Anisoara Paraschiv-Ionescu, Martin Ullrich, Cameron Kirk, Abolfazl Soltani, Arne Küderle, et al. «Assessing Real-World Gait with Digital Technology? Validation, Insights and Recommendations from the Mobilise-D Consortium». In: *Journal of NeuroEngineering and Rehabilitation* 20.1 (2023), p. 78. DOI: 10.1186/s12984-023-01198-5 (cit. on pp. 3, 4, 16–19, 35, 36, 62, 63).

[9] Richard Baker. «Gait analysis methods in rehabilitation». In: *Journal of NeuroEngineering and Rehabilitation* 3 (2006), p. 4. DOI: 10.1186/1743-0003-3-4 (cit. on pp. 6, 10, 12).

[10] Jacquelin Perry and Judith M. Burnfield. *Gait Analysis: Normal and Pathological Function*. 2nd ed. Thorofare, NJ: SLACK Incorporated, 2010. ISBN: 9781556427664 (cit. on pp. 6–8).

[11] David Levine, Jim Richards, and Michael W. Whittle, eds. *Whittle's Gait Analysis*. 5th ed. Edinburgh: Churchill Livingstone/Elsevier, 2012. ISBN: 9780702042652 (cit. on pp. 6–8).

[12] Stephanie Studenski et al. «Gait Speed and Survival in Older Adults». In: *JAMA* 305.1 (2011), pp. 50–58. DOI: 10.1001/jama.2010.1923 (cit. on p. 6).

[13] Marilyn MacKay-Lyons. «Central Pattern Generation of Locomotion: A Review of the Evidence». In: *Physical Therapy* 82.1 (2002), pp. 69–83. DOI: 10.1093/ptj/82.1.69 (cit. on p. 7).

[14] Volker Dietz. «Spinal Cord Pattern Generators for Locomotion». In: *Clinical Neurophysiology* 114.8 (2003), pp. 1379–1389. DOI: 10.1016/S1388-2457(03)00120-2 (cit. on p. 7).

[15] Alvaro Muro-de-la-Herran, Begonya Garcia-Zapirain, and Amaia Mendez-Zorrilla. «Gait Analysis Methods: An Overview of Wearable and Non-Wearable Systems, Highlighting Clinical Applications». In: *Sensors* 14.2 (2014), pp. 3362–3394. DOI: 10.3390/s140203362 (cit. on pp. 10, 14).

[16] Aurelio Cappozzo, Ugo Della Croce, Alberto Leardini, and Lorenzo Chiari. «Human Movement Analysis Using Stereophotogrammetry. Part 1: Theoretical Background». In: *Gait & Posture* 21.2 (2005), pp. 186–196 (cit. on pp. 10, 11).

[17] Gayatri Suresh. *An Introduction to Gait Analysis*. Dec. 2022. URL: https://auptimo.com/an-introduction-to-gait-analysis/ (visited on 08/24/2026) (cit. on p. 12).

[18] Francesca Salis, Stefano Bertuletti, Tecla Bonci, Ugo Della Croce, Claudia Mazzà, and Andrea Cereatti. «A Method for Gait Events Detection Based on Low Spatial Resolution Pressure Insoles Data». In: *Journal of Biomechanics* 127 (2021), p. 110687. DOI: 10.1016/j.jbiomech.2021.110687 (cit. on pp. 13, 23).

[19] Francesca Salis, Stefano Bertuletti, Tecla Bonci, Marco Caruso, Kirsty Scott, Lisa Alcock, et al. «A multi-sensor wearable system for the assessment of diseased gait in real-world conditions». In: *Frontiers in Bioengineering and Biotechnology* 11 (2023), p. 1143248. DOI: 10.3389/fbioe.2023.1143248 (cit. on pp. 13, 20–24, 34).

[20] Angelo Maria Sabatini. «Estimating Three-Dimensional Orientation of Human Body Parts by Inertial/Magnetic Sensing». In: *Sensors* 11.2 (2011), pp. 1489–1525. DOI: 10.3390/s110201489 (cit. on pp. 13, 16).

[21] Zainab Mohammed, Ibrahim M. Elfadel, and Mahmoud Rasras. «Monolithic Multi Degree of Freedom (MDoF) Capacitive MEMS Accelerometers». In: *Micromachines* 9.11 (2018), p. 602. DOI: 10.3390/mi9110602 (cit. on p. 14).

[22] Demoz Gebre-Egziabher, Gabriel H. Elkaim, J. David Powell, and Bradford W. Parkinson. «Calibration of Strapdown Magnetometers in Magnetic Field Domain». In: *Journal of Aerospace Engineering* 19.2 (2006), pp. 87–102 (cit. on p. 16).

[23] Eleftheria Giannouli, Otmar Bock, Sabato Mellone, and Wiebren Zijlstra. «Mobility in Old Age: Capacity Is Not Performance». In: *BioMed Research International* 2016 (2016), p. 3261567. DOI: 10.1155/2016/3261567 (cit. on pp. 16, 17).

[24] World Health Organization. *International Classification of Functioning, Disability and Health: ICF*. Geneva: World Health Organization, 2001. ISBN: 9789241545426 (cit. on p. 17).

[25] Akira Matsushima, Kunihiro Yoshida, Hirokazu Genno, and Shu-ichi Ikeda. «Principal Component Analysis for Ataxic Gait Using a Triaxial Accelerometer». In: *Journal of NeuroEngineering and Rehabilitation* 14.1 (2017), p. 37. DOI: 10.1186/s12984-017-0249-7 (cit. on p. 18).

[26] Vrutangkumar V. Shah et al. «Gait Variability in Spinocerebellar Ataxia Assessed Using Wearable Inertial Sensors». In: *Movement Disorders* 36.12 (2021), pp. 2922–2931. DOI: 10.1002/mds.28740 (cit. on p. 18).

[27] Vrutangkumar V. Shah et al. «Clinic vs. Daily Life Gait Characteristics in Patients with Spinocerebellar Ataxia». In: *Frontiers in Digital Health* 7 (2025), p. 1590150. DOI: 10.3389/fdgth.2025.1590150 (cit. on pp. 19, 67).

[28] Tine Alkjær, Peter K. Larsen, Gitte Pedersen, Linda H. Nielsen, and Erik B. Simonsen. «Biomechanical analysis of rollator walking». In: *BioMedical Engineering OnLine* 5 (2006), p. 2. DOI: 10.1186/1475-925X-5-2 (cit. on p. 64).

[29] Francesca Salis, Stefano Bertuletti, Kirsty Scott, Marco Caruso, Tecla Bonci, Ellen Buckley, Ugo Della Croce, Claudia Mazzà, and Andrea Cereatti. «A Wearable Multi-Sensor System for Real-World Gait Analysis». In: *2021 43rd Annual International Conference of the IEEE Engineering in Medicine and Biology Society (EMBC)*. IEEE, 2021, pp. 7020–7023. DOI: 10.1109/EMBC46164.2021.9630392 (cit. on pp. 20–22).

[30] Claudia Mazzà, Lisa Alcock, Kamiar Aminian, Clemens Becker, Stefano Bertuletti, Tecla Bonci, et al. «Technical Validation of Real-World Monitoring of Gait: A Multicentric Observational Study». In: *BMJ Open* 11.12 (2021), e050785. DOI: 10.1136/bmjopen-2021-050785 (cit. on p. 20).

[31] Stefano Bertuletti, Andrea Cereatti, Daniele Comotti, Michele Caldara, and Ugo Della Croce. «Static and Dynamic Accuracy of an Innovative Miniaturized Wearable Platform for Short Range Distance Measurements for Human Movement Applications». In: *Sensors* 17.7 (2017), p. 1492. DOI: 10.3390/s17071492 (cit. on p. 24).

[32] Axivity Ltd. *AX6: 6-Axis Logging Accelerometer*. URL: https://axivity.com/product/ax6 (visited on 08/11/2026) (cit. on p. 25).

[33] Mahmoud El-Gohary, Sean Pearson, James McNames, Martina Mancini, Fay Horak, Sabato Mellone, and Lorenzo Chiari. «Continuous Monitoring of Turning in Patients with Movement Disability». In: *Sensors* 14.1 (2014), pp. 356–369. DOI: 10.3390/s140100356 (cit. on p. 35).

[34] Arne Küderle, Annika Mücke, Chloe Hinchliffe, Dimitrios Megaritis, Paolo Tasca, Zamal Ali, Felix Kluge, and Alexandru Stihi. *MobGap: The Mobilise-D Algorithm Toolbox*. 2024. DOI: 10.5281/zenodo.14035833 (cit. on p. 34).

[35] Khaireddine Ben Mansour, Nasser Rezzoug, and Philippe Gorce. «Foot side detection from lower lumbar spine acceleration». In: *Gait & Posture* 42.3 (2015), pp. 386–389. DOI: 10.1016/j.gaitpost.2015.05.021 (cit. on p. 35).

[36] Minh H. Pham et al. «Validation of a Step Detection Algorithm during Straight Walking and Turning in Patients with Parkinson's Disease and Older Adults Using an Inertial Measurement Unit at the Lower Back». In: *Frontiers in Neurology* 8 (2017), p. 457. DOI: 10.3389/fneur.2017.00457 (cit. on pp. 40, 64).

[37] Alexander Kvist, Fredrik Tinmark, Lucian Bezuidenhout, Mikael Reimeringer, David Moulaee Conradsson, and Erika Franzén. «Validation of algorithms for calculating spatiotemporal gait parameters during continuous turning using lumbar and foot mounted inertial measurement units». In: *Journal of Biomechanics* 162 (2024), p. 111907. DOI: 10.1016/j.jbiomech.2023.111907 (cit. on pp. 40, 64).

[38] Cameron Kirk, Arne Küderle, M. Encarna Micó-Amigo, et al. «Mobilise-D insights to estimate real-world walking speed in multiple conditions with a wearable device». In: *Scientific Reports* 14 (2024), p. 1754. DOI: 10.1038/s41598-024-51766-5 (cit. on pp. 62, 63).

[39] Abolfazl Soltani, Kamiar Aminian, Claudia Mazza, Andrea Cereatti, Luca Palmerini, Tecla Bonci, and Anisoara Paraschiv-Ionescu. «Algorithms for Walking Speed Estimation Using a Lower-Back-Worn Inertial Sensor: A Cross-Validation on Speed Ranges». In: *IEEE Transactions on Neural Systems and Rehabilitation Engineering* 29 (2021), pp. 1955–1964. DOI: 10.1109/TNSRE.2021.3111681 (cit. on p. 63).

[40] Luca Palmerini et al. «Mobility recorded by wearable devices and gold standards: the Mobilise-D procedure for data standardization». In: *Scientific Data* 10 (2023), p. 38. DOI: 10.1038/s41597-023-01930-9 (cit. on p. 65).

[41] Massimiliano Pau, Micaela Porta, Chiara Pau, Paolo Tacconi, and Angela Sanna. «Quantitative Characterization of Gait Patterns in Individuals with Spinocerebellar Ataxia 38». In: *Bioengineering* 10.7 (2023), p. 788. DOI: 10.3390/bioengineering10070788 (cit. on p. 66).

[42] Hannah L. Casey et al. «Gait characteristics in people with Friedreich ataxia: daily life versus clinic measures». In: *Frontiers in Neurology* 16 (2025), p. 1544453. DOI: 10.3389/fneur.2025.1544453 (cit. on p. 66).